



1 **How does water yield respond to mountain pine beetle infestation in a**
2 **semiarid forest?**

3 Jianning Ren^{1,3}, Jennifer Adam¹, Jeffrey A. Hicke², Erin Hanan³, Naomi Tague⁴, Mingliang Liu¹,
4 Crystal Kolden⁵, John T. Abatzoglou⁵

5

6 ¹ Department of Civil & Environmental Engineering, Washington State University, 99163,
7 Pullman, USA

8 ² Department of Geography, University of Idaho, 83844, Moscow, USA

9 ³ Department of Natural Resources and Environmental Sciences, University of Nevada, 89501,
10 Reno, USA

11 ⁴ Bren School of Environmental Science & Management, University of California, 93106, Santa
12 Barbara, USA

13 ⁵ Management of Complex Systems, University of California, 95344, Merced, USA

14

15 *Corresponding to: Jennifer Adam (jcadam@wsu.edu)*

16

17

18

19



20 **Key points:**

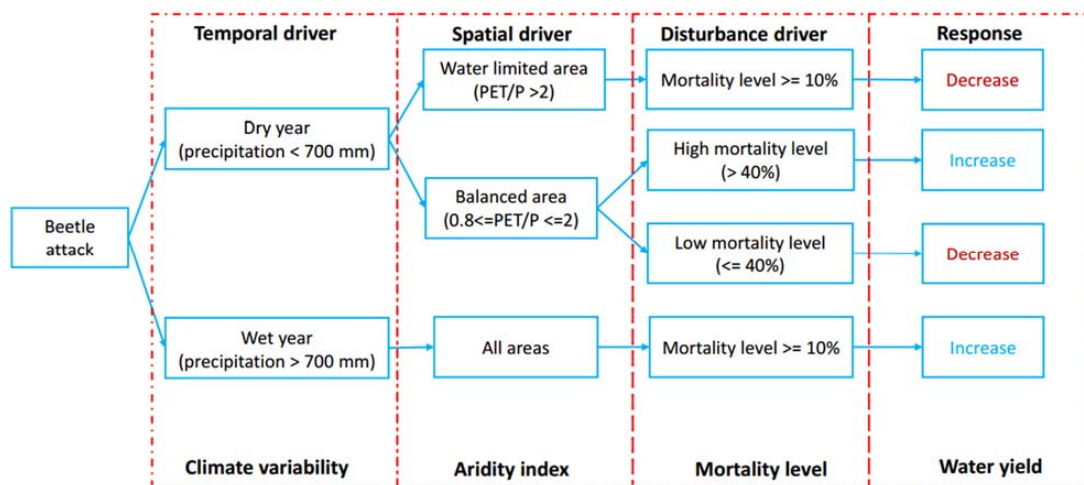
- 21 • Mountain pine beetle (MPB)-caused tree mortality increases water yield in most wet
22 years, and a decrease in water yield mainly happens in dry years; therefore, interannual
23 climate variability is an important driver of water yield response to beetle-caused tree
24 mortality.
- 25 • A long-term (multi-decade) aridity index is a reliable indicator of water yield response to
26 MPBs: in a dry year, decreases occur mainly in “water-limited” areas and vegetation
27 mortality levels have only minor effects; in wetter areas, decreases only occur at low
28 mortality levels.
- 29 • Generally, in a dry year, low to medium MPB-caused vegetation mortality decreases
30 water yield, and high mortality increases water yield; this response to mortality level is
31 nonlinear and varies by location and year.

32

33



34 Graphical abstract



35

36 Abstract

37 Mountain pine beetle (MPB) outbreaks in western United States result in widespread tree
38 mortality, transforming forest structure within watersheds. While there is evidence that these
39 changes can alter the timing and quantity of streamflow, there is substantial variation in both the
40 magnitude and direction of responses and the climatic and environmental mechanisms driving
41 this variation are not well understood. Herein, we coupled an eco-hydrologic model (RHESys)
42 with a beetle effects model and applied it to a semiarid watershed, Trail Creek, in the Bigwood
43 River basin in central Idaho to evaluate how varying degrees of beetle-caused tree mortality
44 influence water yield. Simulation results show that water yield during the first 15 years after
45 beetle outbreak is controlled by interactions among interannual climate variability, the extent of
46 vegetation mortality, and long-term aridity. During wet years, water yield after beetle outbreak
47 increases with greater tree mortality. During dry years, water yield decreases at low to medium
48 mortality but increases at high mortality. The mortality threshold for the direction of change is



49 location-specific. The change in water yield also varies spatially along aridity gradients during
50 dry years. In relatively wetter areas of the Trail Creek basin, water yield switches from a
51 decrease to an increase when vegetation mortality is greater than 40 percent. In more water-
52 limited areas on the other hand, water yield typically decreases after beetle outbreaks, regardless
53 of mortality level. Results suggest that long-term aridity can be a useful indicator for the
54 direction of water yield changes after disturbance.

55 **1 Introduction**

56 In recent decades, mountain pine beetle (MPB) outbreaks in the Western U.S. and Canada have
57 killed billions of coniferous trees (Bentz et al. 2010). Coniferous forests can provide essential
58 ecosystem services, including water supply for local communities (Anderegg et al. 2013).
59 Therefore, it is essential to understand how ecosystems and watersheds respond to beetle
60 outbreaks and to identify the dominant processes that drive these responses (Bennett et al. 2018).
61 A growing number of studies have qualitatively examined hydrologic responses to beetle
62 outbreaks and disturbance; however these studies have produced conflicting results (Adams et al.
63 2012; Goeking and Tarboton 2020). While some studies show increases in water yield following
64 beetle outbreak (e.g., Bethlahmy 1974; Potts 1984; Livneh et al. 2015), many others show no
65 change or even decreases (e.g., Guardiola-Claramonte et al. 2011; Biederman et al. 2014; Slinski
66 et al. 2016). To determine which mechanisms control change in water yield following beetle
67 outbreak, more quantitative approaches are needed.

68 Water yield is often thought to increase after vegetation is killed or removed by disturbances
69 such as fire, thinning, and harvesting (Hubbart 2007; Robles et al. 2014; Chen et al. 2014; Buma
70 and Livneh 2017; Wine et al. 2018). In the Rocky Mountain West, beetle outbreaks have
71 increased water yield through multiple mechanisms. First, defoliation/needle loss can reduce



72 plant transpiration, canopy evaporation, and canopy snow sublimation losses to the atmosphere
73 (Montesi et al. 2004). Increased canopy openings can also enable snow accumulation and allow
74 more radiation to reach the ground surface, resulting in earlier and larger peak snowmelt events,
75 which can in turn reduce soil moisture and therefore decrease summer evapotranspiration (ET).
76 Several studies have documented decreases in water yield following disturbances (e.g., mortality,
77 fire, beetle outbreaks; Biederman et al. 2014; Bart et al. 2016; Slinski et al. 2016; Goeking and
78 Tarboton 2020). For example, in the southwestern U.S., beetle outbreaks have decreased
79 streamflow by opening forest canopies and increasing radiation to the understory and at the
80 ground surface, which leads to increases in understory vegetation transpiration (Guardiola-
81 Claramonte et al. 2011), soil evaporation, and therefore increases total ET (Bennett et al. 2018).
82 Tree mortality or removal can reduce streamflow because surviving trees and/or understory
83 vegetation compensates by using more water (Tague et al. 2019).

84 In a review of 78 studies, Goeking and Tarboton (2020) concluded that the decrease in water
85 yield after tree-mortality mainly happens in semiarid regions. Previous studies also provide rule-
86 of-thumb thresholds above which water yield will increase: at least 20 percent loss of vegetation
87 cover and mean precipitation of 500 mm/year (Adams et al. 2012). However, many watersheds
88 in the western U.S. experience high interannual climate variability (Fyfe et al. 2017), and local
89 environmental gradients (e.g., long-term aridity gradients) may strongly influence vegetation and
90 hydrologic responses to disturbances, including beetle outbreaks, making predictions difficult
91 (Winkler et al. 2014). Given the possibility of either increases or decreases in water yield
92 following beetle outbreaks, modeling approaches are crucial for identifying the specific
93 mechanisms that control these responses.



94 The overarching goal of this study is to identify mechanisms driving the direction of change in
95 annual water yield after beetle outbreaks in semi-arid regions (note that in the following text,
96 “water yield” refers to means annual water yield). The following specific questions address this
97 goal:

- 98 • **Q1:** What is the role of **interannual climate variability** in water yield response?
- 99 • **Q2:** What is the role of **mortality level** in water yield response?
- 100 • **Q3:** How does **long-term aridity** (defined as temporally averaged potential
101 evapotranspiration relative to precipitation for a period of 38 years) modify these
102 responses, and how do responses vary spatially within a watershed along aridity
103 gradients?

104 We hypothesize that multiple ecohydrologic processes (e.g., snow accumulation and melt,
105 evaporation, transpiration, drainage, and a range of forest structural and functional responses to
106 beetles) could interactively influence how water yield responds to beetle outbreaks—however, in
107 certain locations one or more processes may dominate. In addition, the dominant ecohydrologic
108 processes may vary over space and time due to interannual climate variability (i.e.,
109 precipitation), vegetation mortality, and long-term aridity. In Sect 2, we present a conceptual
110 framework for identifying and depicting dominant hydrological processes through which forests
111 respond to beetle infestation. We use this framework to interpret the modeling results. In Sect 3,
112 we describe our mechanistic modeling approach, i.e., using the Regional Hydro-Ecological
113 Simulation System (RHESSys), which can prescribe a range of vegetation mortality levels,
114 capture the effects of landscape heterogeneity and the role of lateral soil moisture redistribution,
115 and project ecosystem carbon and nitrogen dynamics, including post-disturbance plant recovery.



116 In Sects 4 and 5, we then present modeling results that explore how multiple mechanisms
117 influence water yield responses.

118 **2 Conceptual framework**

119 2.1 Vegetation response to beetle outbreaks

120 Mountain pine beetles (MPB) introduce blue stain fungi into the xylem of attacked trees, which
121 reduces water transport in plants and eventually shuts it off (Paine et al. 1997). During outbreaks,
122 MPBs prefer to attack and kill larger host trees that have greater resources (e.g., carbon), while
123 smaller diameter host trees and non-host vegetation (including the understory) remain unaffected
124 (Edburg et al. 2012). After MBP outbreak, trees mainly go through three phases (i.e., red, gray,
125 and old) over time (Hicke et al. 2012). During the red phase, the trees' needles turn red. During
126 the gray phase, there are no needles in the canopy. During old phase, killed trees have fallen, and
127 understory vegetation and new seedlings experience rapid growth (Hicke et al. 2012; Mikkelsen
128 et al. 2013).

129 2.2 Hydrologic response to beetle outbreaks

130 Figure 1 describes the main processes that alter evapotranspiration to either decrease or increase
131 water yield, depending on which processes dominate (Adams et al. 2012; Goeking and Tarboton
132 2020). During the red and gray phases, needles fall to the ground, and there is lower leaf area
133 index (LAI) and a more open canopy (Hicke et al. 2012). This can reduce plant transpiration of
134 infected trees, though remaining trees may compensate to some extent by increasing
135 transpiration in water limited environments (Adams et al. 2012, Tague et al. 2019). A more open
136 canopy intercepts less precipitation, reducing evaporation from the canopy but potentially
137 increasing it from soil and litter layers (Montesi et al. 2004; Sexstone et al. 2018). Meanwhile, an
138 open canopy can increase the proportion of snow falling to the ground and, therefore, increase



139 snowpack accumulation. With more solar radiation reaching the ground, earlier and larger peak
140 snowmelt can also occur (Bennett et al. 2018). Generally, earlier snowmelt increases water for
141 spring streamflow and decreases water for summertime ET (Pomeroy et al. 2012). However,
142 once snags fall, reductions in longwave radiation can actually lead to later snowmelt (Lundquist
143 et al. 2013). The open canopy and less competition for resources, such as solar radiation and
144 nutrients, can also promote understory vegetation growth, which may increase understory
145 transpiration (Biederman et al. 2014; Tague et al. 2019). Whether water yield increases or
146 decreases will ultimately depend on the balance of these processes that can alter transpiration and
147 evaporation in different ways.

148

149 Finally, interannual variability in climate (e.g., dry versus wet years) can affect forests'
150 hydrological responses (Winkler et al. 2014; Goeking and Tarboton 2020). For instance, during
151 wet years, remaining plants are not water-limited, and reductions in plant transpiration due to
152 beetle-caused mortality dominate increases in soil evaporation or remaining plant transpiration,
153 resulting in a higher water yield. In contrast, during dry years, plants are already under water
154 stress and decreases in plant transpiration caused by tree mortality may be compensated by
155 increasing soil evaporation and transpiration by remaining trees or understory vegetation, leading
156 to declines in water yield. Moreover, these responses are also affected by land cover types (e.g.,
157 young vs old pine, different tree species, etc.), which is not currently well documented (Perry
158 and Jones 2017; Morillas et al. 2017).

159 2.3 Review of modeling approaches

160 Many models, ranging from empirical and lumped to physically-based and fully-distributed,
161 have been used to study hydrologic responses to disturbances. Goeking and Tarboton (2020)



162 argue that only physically-based and fully-distributed models can capture how disturbances alter
163 water yield because they represent fine-scale spatial heterogeneity and physical process that vary
164 over space and time. Despite their advantages, process-based models, such as the coupled CLM-
165 ParFlow model (Mikkelsen et al. 2013; Penn et al. 2016), the Distributed Hydrology Soil
166 Vegetation Model (Livneh et al. 2015; Sun et al. 2018), and the Variable Infiltration Capacity
167 Model (Bennett et al. 2018) also have some limitations. For example, 1) they may assume
168 constant LAI after disturbances and static vegetation growth (e.g., VIC and DHSVM), 2) they
169 may not include lateral flow to redistribute soil moisture (VIC), and 3) in some cases, the
170 approach to represent the effects of beetle outbreaks may be too simplified (e.g., changing only
171 LAI and conductance without considering two-way beetle-vegetation interactions in post-
172 disturbance biogeochemical and water cycling e.g., as in CLM-ParFlow). Thus, improving
173 current fully distributed process-based models to capture the coupled dynamics between
174 hydrology and vegetation at multiple scales is a critical step for projecting how beetle outbreaks
175 will affect water yield in semiarid systems (Goeking and Tarboton 2020). Here we use
176 RHESSys7.1, which captures these processes.

177 **3 Model, data, and simulation experiment design**

178 3.1 Study area

179 Our study watershed is Trail Creek, which is located in Blaine County between the Sawtooth
180 National Forest and the Salmon-Challis National Forest (43.44N, 114.19W; Fig. 2). It is a 167-
181 km² sub-catchment in the south part of Big Wood River basin, and is within the wildland-urban
182 interface where residents are vulnerable to the flood and debris flows caused by forest
183 disturbances (Skinner 2013). Trail Creek has frequently experienced beetle outbreaks, notably in
184 2004 and 2009, when beetles killed 7 and 19 km² of trees, respectively (Berner et al. 2017).



185 Trail Creek has cold, wet winters and warm, dry summers; mean annual precipitation is
186 approximately 978 mm with 60% snow (Frenzel 1989). The soil is mostly permeable coarse
187 alluvium (Smith 1960). Vegetation is clustered into two major groups along the elevation which
188 ranges from 1760 to 3478 m: sagebrush, riparian species, and grasslands in lower to middle
189 elevation areas and Douglas-fir (*Pseudotsuga menziesii*), lodgepole pine (*Pinus contorta* var.
190 *latifolia*), subalpine fir (*Abies lasiocarpa*), and mixed shrub and herbaceous vegetation in
191 middle-to-higher elevations (Buhidar 2002).

192 A strong upper to lower vegetation and long-term aridity gradient exists for Trail Creek (Fig. 3).
193 The northern (higher elevation) portion of the basin is mesic and covered principally by
194 evergreen forest; the southern (lower elevation) portion is xeric and covered by shrubs, grasses,
195 and mixed herbaceous species. In total, Trail creek contains 72 sub-basins and two of them (e.g.,
196 Fig. 3, sub-basin 412 and 416) are urban areas. If we classify this basin into different zones
197 according to an aridity index, i.e., the ratio of 38-year average annual potential
198 evapotranspiration (PET) to precipitation (P) (Sect 3.4), there is a distinct gradient: the northern
199 and high elevation area is balanced (i.e., PET/P between 0.8 and 2) and evergreen tree coverage
200 is more than 50%; the southern part is water-limited (i.e., PET/P > 2) and evergreen tree
201 coverage is less than 30% (Figs. 2 and 3).

202 3.2 Model descriptions

203 3.2.1 Ecohydrologic model

204 The Regional Hydro-ecologic Simulation System (RHESSys) (Tague and Band 2004) is a
205 mechanistic model designed to simulate the effects of climate and land use change on ecosystem
206 carbon and nitrogen cycling and hydrology. RHESSys fully couples hydrological processes
207 (including streamflow, lateral flow, ET, and soil moisture, etc.), plant growth and vegetation



208 dynamics (including photosynthesis, maintenance respiration, and mortality, etc.), and soil
209 biogeochemical cycling (including soil organic matter decomposition, mineralization,
210 nitrification, denitrification, and leaching, etc.). It has been widely tested and applied in several
211 mountainous watersheds in western North America, including many in the Pacific and Inland
212 Northwest (e.g., Tague and Band 2004; Garcia and Tague 2015; Hanan et al. 2017; Hanan et al.
213 2018; Lin et al. 2019; Son and Tague 2019).

214 RHESSys represents a watershed using a hierarchical set of spatial units, including patches,
215 zones, sub-basins, and the full basin, to simulate various hydrologic and biogeochemical
216 processes occurring in these multiple scales (Tague and Band 2004). The patch is the finest
217 spatial scale at which vertical soil moisture and soil biogeochemistry are simulated. In every
218 patch, there are multiple canopy strata layers to simulate the biogeochemical processes related to
219 plant growth and nutrient uptake. Meteorological forcing inputs (e.g., temperature, precipitation,
220 humidity, wind speed, and solar radiation) are handled at the zone level, and spatially
221 interpolated and downscaled for each patch based on elevation, slope, and aspect. Sub-basins are
222 closed drainage areas entering both sides of a single stream reach (the water budget is closed in
223 sub-basins). The largest spatial unit is the basin, which aggregates the streamflow from sub-
224 basins (Tague and Band 2004; Hanan et al. 2018). In RHESSys, streamflow is the sum of
225 overland flow and baseflow, and we consider streamflow as the *water yield* of each sub-basin.

226 RHESSys models vertical and lateral hydrologic fluxes, including canopy interception, plant
227 transpiration, canopy evaporation/sublimation, snow accumulation, snowmelt and sublimation,
228 soil evaporation, soil infiltration, and subsurface drainage. Canopy interception is based on the
229 water-holding capacity of vegetation, which is also a function of plant area index (PAI). Both the
230 canopy evaporation and transpiration are modeled using the standard Penman-Monteith equation



231 (Monteith 1965). Snow accumulation is calculated from incoming precipitation and is assumed
232 to fall evenly across each zone. Snowmelt is based on a quasi-energy budget approach
233 accounting for radiation input, sensible and latent heat fluxes, and advection. Soil evaporation is
234 constrained by both energy and atmospheric drivers, as well as a maximum exfiltration rate,
235 which is controlled by soil moisture (Tague and Band 2004). Vertical drainage and lateral flow is
236 a function of topography and soil hydraulic conductivity, which decays exponentially with depth
237 (Tague and Band 2004; Hanan et al. 2018).

238 Vegetation carbon and nitrogen dynamics are calculated separately for each canopy layer within
239 each patch, while soil and litter carbon and nitrogen cycling are simulated at the patch level.
240 Photosynthesis is calculated based on the Farquhar model considering the limitations of nitrogen,
241 light, stomatal conductance (which is influenced by soil water availability), vapor pressure
242 deficit, atmospheric CO₂ concentration, radiation, and air temperature (Farquhar and von
243 Caemmerer 1982; Tague and Band 2004). Maintenance respiration is based on Ryan (1991),
244 which computes respiration as a function of nitrogen concentration and air temperature. Growth
245 respiration is calculated as a fixed ratio of new carbon allocation for each vegetation component
246 (Ryan 1991; Tague and Band 2004). Net photosynthesis is allocated to leaves, stems, and roots at
247 daily steps based on the Dickinson partitioning method, which varies with each plant
248 development stage (Dickinson et al. 1998). LAI is estimated from leaf carbon and specific leaf
249 area for each vegetation type. The soil and litter carbon and nitrogen cycling (heterotrophic
250 respiration, mineralization, nitrification, and denitrification, etc.) are modified from the
251 BIOME_BGC and CENTURY-NGAS models (White and Running 1994; Parton et al. 1996;
252 Tague and Band 2004). A detailed description of RHESSys model algorithms can be found in
253 Tague and Band (2004).



254 3.2.2 Beetle effects model

255 Edburg et al. (2012) designed and developed a model of MPB effects on carbon and nitrogen
256 dynamics for integration with the Community Land Model Version 4 (CLM4) (Lawrence et al.
257 2011, Fig. 4). Here we integrated this beetle effects model into RHESSys (Fig. 4). Beetles attack
258 trees mainly during late summer, and needles will turn from green to red at the beginning of the
259 following summer. We simplify this process with prescribed tree mortality on September 1 to
260 represent a beetle outbreak of the current year. The advantage of this integration is that RHESSys
261 accounts for the lateral connectivity in water and nitrogen fluxes among patches which is not
262 represented in CLM4 (Fan et al. 2019). Differences in our approach compared to other
263 hydrological models of beetle effects (e.g., VIC, CLM-ParFlow, and DHSVM) include dynamic
264 changes in plant carbon and nitrogen cycling caused by beetle attack, plant recovery, and effects
265 on hydrological responses. Previous studies of hydrologic effects of beetle outbreaks have
266 mainly focused on consequences of changes in LAI and stomatal resistance during each phase of
267 beetle outbreak but have missed feedbacks between carbon and nitrogen dynamics, vegetation
268 recovery, and hydrology (Mikkelson et al. 2013; Livneh et al. 2015; Penn et al. 2016; Sun et al.
269 2018; Bennett et al. 2018).

270 To better represent the effects of beetle-caused tree mortality, we added a snag pool (standing
271 dead tree stems) and a dead foliage pool (representing the red needle phase) in RHESSys (Fig.
272 4). All leaf biomass (including carbon and nitrogen) become part of dead foliage pools. After one
273 year (Hicke et al. 2012; Edburg et al. 2011) the dead foliage is transferred to litter pools at an
274 exponential rate with a half-life of two years (Edburg et al. 2012). Similarly, stem carbon and
275 nitrogen are moved to the snag pool immediately after outbreak. After five years (Edburg et al.
276 2012), carbon and nitrogen in snags begin to move into the coarse woody debris (CWD) pool at



277 an exponential decay rate with a half-life of ten years (Edburg et al. 2011). After outbreak, the
278 coarse root pools that are killed move to the CWD and fine root pools move to litter pools. To
279 simplify, we assume a uniform mortality level for all evergreen patches across landscape. Due to
280 the limitation of land cover data, we cannot separate pine and fir in these evergreen patches.
281 However, this will not affect the interpretation of our results because we analyze them based on
282 mortality level and evergreen vegetation coverage rather than different species.

283 In the integrated model, the reduction of leaf carbon and nitrogen after beetle outbreak can
284 directly decrease LAI and canopy height, which consequently affects energy (i.e., longwave
285 radiation and the interception of shortwave radiation) and hydrologic (i.e., transpiration and
286 canopy interception) fluxes. We calculate two types of LAI: **Live LAI** (i.e., only live leaf is
287 included), and **Total LAI** (i.e., both live and dead leaves are included). The calculation of plant
288 transpiration is based on Live LAI, while the calculation of other canopy properties, including
289 interception and canopy evaporation, is based on Total LAI. The calculation of canopy height
290 includes the living stem and the snag pool.

291 3.3 Input data

292 We used the US Geologic Survey (USGS) National Elevation Dataset (NED) at 10 m resolution
293 to calculate the topographic properties of Trail Creek, including elevation, slope, aspect, basin
294 boundaries, sub-basins, and patches. Using NED, we delineated 16705 100-m resolution patches
295 within 72 sub-basins. We used the National Land Cover Database (NLCD) to identify five
296 vegetation and land cover types, i.e., evergreen, grass/herbaceous, shrub, deciduous, and urban
297 (Homer et al. 2015). We determined soil properties for each patch using the POLARIS database
298 (probabilistic remapping of SSURGO; Chaney et al. 2016). Parameters for soil and vegetation



299 were based on previous research and literature (White et al. 2000; Law et al. 2003; Ackerly
300 2004; Berner and Law 2016; Hanan et al. 2016).

301 Climate inputs for this study, including maximum and minimum temperatures, precipitation,
302 relative humidity, radiation, and wind speed, were acquired from gridMET for years from 1980
303 to 2018. GridMET provides daily high-resolution (1/24 degree or ~4 km) gridded meteorological
304 data (Abatzoglou 2013). It is a blended climate dataset that combines the temporal attributes of
305 gauge-based precipitation data from NLDAS-2 (Mitchell et al. 2004) with the spatial attributes of
306 gridded climate data from PRISM (Daly et al. 1994).

307 3.4 Simulation experiments

308 To quantify how water yield responds to beetle-caused mortality, we designed the following
309 simulation experiment. We prescribed a beetle outbreak in September 1989, the mortality level
310 (%) is applied to all evergreen patches for each sub-basin. After beetle outbreak, red needles stay
311 on the trees for one year before they start to fall (transferred to the litter pool) at an exponential
312 rate with a half-life of two years. The snag pools stay in the standing trees for five years and then
313 start to fall and are added to the CWD pool which decays at an exponential rate with a half-life
314 of ten years.

315 To address Q1 (i.e., the role of interannual variability), we compared water yield responses
316 during a dry water year, 1994 (i.e., five years after beetle outbreak with precipitation 611 mm),
317 to responses during a wet year, 1995 (i.e., six years after beetle outbreak with precipitation 1394
318 mm). This enabled us to estimate the role of interannual climate variability in driving changes in
319 water yield following beetle attack. The dry year are selected based on years that have
320 precipitation below the 15th percentile across 38 years of annual precipitation data (from 1979 to
321 2017) (Searcy 1959, see Fig. S1). During these early period after beetle outbreak (e.g., 1994 and



1995) the forest is experiencing large changes in vegetation canopy cover, plant transpiration, and soil moisture. We chose these two successive years because they have almost similar canopy and vegetation status in terms of fallen dead foliage and residual vegetation regrowth, which makes this comparison reasonable. However, it is possible that antecedent climate conditions may affect the following year's response. For example, soil moisture can be depleted during a drought year, affecting initial conditions the following year. Moreover, under drought conditions, less reactive nitrogen is taken up by the plants or leaching is reduced, so more nitrogen will be left for the following year. Therefore, the difference in water yield responses between 1994 and 1995 might be affected by not only climate variations but also initial conditions in the hydrology and the biogeochemistry. To consider the time lag effect (antecedent conditions affecting the current year's response), we also analyzed other dry and wet years.

To address Q2 (i.e., the role of vegetation mortality), we prescribe a range of infestation-caused mortality levels (i.e., from 10% to 60% by a step of 10% in terms of carbon, uniformly applied to all evergreen patches for each sub-basins) and a control run (no mortality) to quantify the response of forests in water yield to vegetation mortality level (for each sub-basin **vegetation mortality is evergreen mortality** multiplied by evergreen coverage of that basin). The differences in water yield between each mortality level and the control run represent the effects of beetle kill: a positive value means that mortality increased water yield, and vice versa.

We quantified the water budget for each sub-basin to examine which hydrological process contribute to the water yield responses: water yield (Q), precipitation (P), canopy evaporation (E_{canopy} , canopy evaporation and snow sublimation), transpiration (T), ground evaporation (E_{ground} , includes bare soil evaporation, pond evaporation, and litter evaporation), snow sublimation (Sublim, ground), soil storage change (dS_{soil}/dt), litter storage change



345 $(\frac{dS_{litter}}{dt})$, snowpack storage change $(\frac{dS_{snowpack}}{dt})$ and canopy storage change
346 $(\frac{dS_{canopy}}{dt})$.

347 The storage components include soil, litter, and canopy. According to Eq. (1), if the storage
348 increases, water yield decreases.

349
$$Q = P - E_{canopy} - E_{ground} - Sublim -$$

350
$$T - \frac{d(S_{soil} + S_{litter} + S_{canopy} + S_{snowpack})}{dt} \quad (1)$$

351 Calculating water balance differences between different mortality scenarios and control scenario
352 results in Eq. (2):

353
$$\Delta Q = \Delta E_{canopy} + \Delta E_{ground} + \Delta Sublim + \Delta T +$$

354
$$\Delta \left(\frac{d(S_{soil} + S_{litter} + S_{canopy} + S_{snowpack})}{dt} \right) \quad (2)$$

355 To address Q3 (i.e., the role of long-term aridity), we calculated the long-term aridity index
356 (PET/P, Fig. 3) across the basin and analyzed the relationship between long-term aridity index
357 and hydrologic response. As mentioned earlier, the long-term aridity index is defined as the ratio
358 of mean annual potential ET (PET) to annual precipitation (P), averaged over 38 years (water
359 year 1980-2018) of historical meteorological data. Based on the long-term aridity index, we
360 classified our sub-basins into three types (McVicar et al. 2012, Table 1).

361



362 **4 Results**

363 4.1 Simulated vegetation response to beetle outbreak at basin-scale

364 4.1.1 Vegetation response to beetle outbreaks

365 Figure 5 shows the basin-scale vegetation response after beetle outbreak in 1989. Live LAI
366 dropped immediately after beetle outbreak, then gradually recovered to pre-outbreak levels
367 during following years (Fig. 5a). Total LAI (i.e., including dead foliage) showed a slight increase
368 during the first ten years after beetle outbreak (1990 – 2000), which is due to the retention of
369 dead leaves in the canopy and the simultaneous growth of residual (unaffected) overstory and
370 understory vegetation (Fig. 5b). The dead foliage pool (Fig. 5c) remained in place for one year
371 and then began to fall to ground (converted to litter) exponentially with a half-life of two years,
372 and the snag pool (Fig. 5d) remained in place for five years and then began to fall to ground
373 (converted to CWD) exponentially with a half-life of ten years. These behaviors of the dead
374 foliage and snag pools are similar to Edburg et al. (2012), which demonstrates that the integrated
375 model is simulating expected vegetation dynamics following beetle outbreak.

376 4.1.2 Time series of hydrologic response to beetle outbreak

377 Figure 6 shows the changes in simulated water fluxes and soil moisture over the basin after
378 beetle outbreak with various evergreen mortality levels. During the first 15 years after beetle
379 outbreak, scenarios where the evergreen mortality level was larger than zero had higher basin-
380 scale water yield than the control scenario (where the evergreen mortality level was zero). This
381 was especially true during wet years; however, there was no significant increase during dry years
382 (i.e., 1992, 1994, 2001, and 2004; Fig. 6a). The year-to-year soil storage fluxes responded
383 strongly in the first two years after beetle outbreak, then stabilized to the pre-outbreak condition
384 (Fig. 6b). Note that year-to-year soil storage change is not the same as soil water storage. After



385 beetle outbreak, the soil can hold some portion of water that not being up taken by the plants, but
386 it was confined by the soil water holding capacity. This phenomenon indicates that the soil has
387 some resilience to vegetation change.

388 Beetle outbreaks reduced transpiration during wet years but did not have significant effects in
389 dry years (Fig. 6c). This is because transpiration in dry years was water-limited and so was much
390 lower than the potential rate (more water is partitioned to evaporation; Biederman et al. 2014).
391 Thus, killing more trees had little effect on stand scale transpiration because remaining trees
392 utilized any water released by the dead trees in dry years. On the other hand, plant transpiration
393 in wet years was close to the potential rate; therefore, decreases in canopy cover reduced
394 transpiration. The simulation results did not show any apparent effect on snowmelt after beetle
395 outbreak.

396 The evaporation response was opposite in dry and wet years: evaporation increased in dry years,
397 while it decreased in wet years (Fig. 6d). This phenomenon is caused by tradeoffs and
398 interactions among multiple processes, as will be explained in more detail in the next section.

399 4.2 The role of spatial heterogeneity in water yield response

400 4.2.1 Spatial patterns of hydrologic response along long-term aridity gradient

401 4.2.1.1 Evaporation

402 Beetle outbreak had opposite effects on evaporation between a dry year and a wet year (Fig. 7).
403 In the dry year, most sub-basins experienced higher evaporation for beetle outbreak scenarios
404 than in the control scenario (Fig. 7a). This was the cumulative consequence of decreased canopy
405 evaporation and increased ground (soil, litter, pond) evaporation due to decreases in LAI (caused
406 by mortality). In the dry year, the latter effect (i.e., increased ground evaporation) dominated



407 over the former effect so that overall consequence was increased evaporation. When the
408 vegetation mortality level (calculated as *the percentage of evergreen patches in a sub-basin*
409 *multiplied by the mortality level of evergreen caused by beetles*) was higher than 20%, a few sub-
410 basins in the balanced (more mesic) area showed some decrease, indicating that the effects of
411 decreasing canopy evaporation exceeded the effects of increasing ground evaporation. In the wet
412 year, most of the sub-basins located in the balanced area showed decreases in evaporation, and
413 the decreasing trend showed linear relationship with vegetation mortality level (where canopy
414 evaporation decreases are dominant, Fig. 7b). However, sub-basins located in much drier regions
415 (aridity >3.5) had relatively insignificant responses to vegetation mortality levels and some of
416 them even had slight increases in evaporation (where ground evaporation increases are dominant
417 due to drier long-term climate and less pine coverage resulted in lower canopy mortality).

418 4.2.1.2 Transpiration

419 Beetle outbreak decreased transpiration in both dry and wet years, and with higher mortality
420 levels the decrease became larger (Fig. 8). However, during the dry year, the water-limited area
421 showed less change than the balanced area; some sub-basins even showed slight increases. This
422 increase in the water-limited part of the basin occurred because after beetles kill some overstory
423 evergreen trees, the living trees and understory plants together can exhibit higher transpiration
424 rates in dry years (Tsamir et al. 2019). In the wet year, when most canopies reach potential
425 transpiration rates (less competition for water), beetle outbreaks can reduce transpiration rates by
426 decreasing Live LAI.

427 4.2.1.3 Total ET



428 Figure 9 depicts the spatial pattern of changes in total ET (i.e., evaporation and transpiration)
429 after beetle outbreak. In a dry year, the balanced and water-limited areas showed opposite
430 responses to mortality: the balanced area showed a decrease in ET and the water-limited area
431 showed a slight increase. In the balanced area, larger ET decreases occurred with higher
432 mortality levels. However, increases in ET in water-limited regions were less sensitive to
433 vegetation mortality level, and even for high vegetation mortality levels (>40%), ET still
434 increased (Fig. 9a). During the wet year, most sub-basins experienced decreasing ET after beetle
435 outbreak and the magnitude was larger with higher vegetation mortality. The different responses
436 of ET were driven by different hydrologic responses (transpiration, ground evaporation and
437 canopy evaporation) competing with each other; this competition was influenced by climate
438 conditions, mortality level, and spatial heterogeneity in long-term aridity.

439 4.2.1.4 Water yield

440 In the dry year (1994), beetle-caused vegetation mortality affected water yield (Fig. 10), but the
441 responses differed between the balanced and water-limited areas. For the **balanced area**, most
442 sub-basins showed slight decreases in water yield after beetle outbreak and no significant
443 differences among low vegetation mortality level ($\leq 40\%$, Fig. 10a). However, with increased
444 mortality levels, more sub-basins showed increases in water yield, particularly with vegetation
445 mortality higher than 40% (Fig. 10a). Moreover, the vegetation mortality threshold that changed
446 the direction of water yield response was altered by long-term aridity, e.g., it was 40% for aridity
447 2.0 but 20% for aridity 1.0. For **the water-limited area**, water yield decreased and was
448 independent from mortality level (Fig. 10a). In the wet year (1995), the water yield in most sub-
449 basins increased after beetle outbreak, and the balanced area increased more significantly than
450 the water-limited area. Furthermore, for the balanced area, higher mortality levels caused larger



451 increases in water yield which responded more linearly (Fig. 10b). In summary, for a wet year,
452 increases in water yield occurred for most sub-basins, driven by a decrease in ET. However,
453 during dry years, the water yield and ET responses were spatially heterogeneous, and the
454 competing changes in evaporation and transpiration changed the direction and magnitude of ET
455 and thus water yield response. The competing effect among different hydrologic fluxes for a dry
456 year is explored in more detail in the next section.

457 4.2.2 Water budgets to understand decreasing water yield in the dry year

458 We analyzed the fluxes in greater detail in a dry year (1994) to understand the response of
459 hydrologic fluxes and resulting water yield. Based on Eq. (2), we identified four hydrological
460 fluxes that can potentially affect water yield: canopy evaporation (canopy evaporation and
461 canopy snow sublimation), ground evaporation (bare soil evaporation, ground snow sublimation,
462 litter evaporation, pond evaporation), plant transpiration, and year-to-year storage change (soil,
463 canopy, litter, snowpack). These three storage terms (canopy, litter, snowpack) were considered
464 together with soil storage since their contribution was minor in comparison with other fluxes.
465 Figure 11 summarized different combinations of these four dominate processes during the dry
466 year (1994) based on their directions (increase or decrease in water yield) after beetle outbreak.
467 In total, fourteen combinations of changes in these fluxes (referred to as “response types”) were
468 found. Five of them resulted in an increase in water yield, and the others resulted in a decrease.

469 Water yield responses caused by the competition of different hydrologic fluxes showed different
470 patterns across the aridity gradient (Figs. 3&10). For the balanced area (upper part of the basin),
471 with low evergreen mortality ($\leq 30\%$), the major response types were D1 and D2, in which the
472 increase in ground evaporation dominated over the decrease in transpiration and canopy
473 evaporation (Fig. 11a, b, and c). However, with higher evergreen mortality ($>30\%$), the major



474 response type became W2, where the increase in ground evaporation did not exceed the decrease
475 in canopy evaporation and transpiration (Fig. 11e, f, and g). This indicates that, in a dry year,
476 when more evergreen stands are killed, the increase in ground evaporation reaches a limit while
477 transpiration and canopy evaporation continue to decrease with decreasing LAI. The increase in
478 ground evaporation was triggered either by decreased Total LAI and open canopy, which
479 allowed more solar radiation penetration to the ground for evaporation (Fig. S5c), or less
480 transpiration from plants, which left more water available to evaporate (Fig. 8a). The decrease in
481 plant transpiration and canopy evaporation was driven by a lower Live LAI and a lower Total
482 LAI, respectively (Fig. S5 a&c and Fig. 8a).

483 The decrease in water yield in the water-limited area (lower part of the basin) was driven by
484 different hydrologic flux competitions in different mortality levels. When evergreen stand
485 mortality level was low ($\leq 30\%$), the response types were D5 and D7, in which the increase in
486 ground and canopy evaporation dominated over the decrease of transpiration (Fig. 11a, b, and c).
487 However, with high evergreen stand mortality ($> 30\%$), the response types became D1 and D2
488 (Fig. 11e, f, and g), in which the canopy evaporation changed from an increase to a decrease that
489 was driven by a decrease in Total LAI (Fig. S5c). When mortality was low, the increases in
490 growth from residual plants and understory outstripped the litter fall of dead foliage; thus, Total
491 LAI increased, and vice versa when mortality was high.

492 **5 Discussion**

493 5.1 Role of interannual climate variability

494 During the first 15 years after beetle attack, various hydrologic processes opposed and/or
495 reinforced one another to either increase or decrease water yield: a decrease in Live LAI can
496 reduce transpiration, while a decrease in Total LAI can enhance ground evaporation but diminish



497 canopy evaporation (Montesi et al. 2004; Tsamir et al. 2019). Interannual climate variability
498 played an important role in determining which of these competing effects dominate and,
499 therefore, drove the direction of water yield response to beetle outbreak (Winkler et al. 2014;
500 Goeking and Tarboton 2020). Our results show that mainly decreases in water yield occurred in
501 dry years, while increases occurred in wet years. During a wet year, plant ET can reach its
502 potential so that any reductions in actual plant ET will dominate over any increases in ground
503 evaporation, resulting in a net increase in water yield. During a dry year, the relative dominance
504 of these competing effects had greater spatial heterogeneity because the water stress status of the
505 plants varied across the basin (as explained in Sect 4.2.2; Fig. 11).

506 However, the responses we observed in the dry year (1994) and in the wet year (1995) were also
507 affected by the previous year's climate (mainly precipitation) and its effects on hydrologic and
508 biogeochemical processes, which set the initial conditions for the dry and wet year (e.g., soil
509 moisture, nitrogen availability, etc.). Therefore, we also analyzed other water years during the
510 first ten years after beetle outbreak to examine whether our findings for dry and wet years follow
511 a general pattern and to what extent they are influenced by antecedent conditions. Results
512 indicate that our findings are robust through the study time period. For example, water yield
513 generally decreased during dry years (1992, 1994, and 2001, see Figs. S1 and S2) and always
514 increased during wet years (1993 and from 1995 to 2000, see Fig. S1 and S2).

515 Adams et al. (2012) provide a threshold of precipitation under which water yield increases after
516 disturbances: at least 500 mm/year (Goeking and Tarboton 2020). The average annual
517 precipitation over this study basin is 600-900 mm in dry years, and higher than 900 mm in wet
518 years. Recent field work observation also find annual climate variability can affect the magnitude
519 of evapotranspiration fluxes that change the water yield direction (Biederman et al. 2014). Our



520 results corroborate these earlier studies by revealing that there are precipitation thresholds above
521 which tree removal increases water yield (Figs. 10, S1 and S2).

522 5.2 Role of vegetation mortality

523 Vegetation mortality is another important factor that influences water yield response. We found
524 that during the wet year, beetle outbreak increased water yield across the basin and the
525 magnitude of these increases grew linearly with the level of vegetation mortality (Fig. 10b). In
526 the dry year, however, the response of water yield to the level of vegetation mortality was more
527 complicated because mortality influenced not only the magnitude of change but also the
528 direction (Fig. 10a). These opposing results (due to mortality level) mainly occurred in the
529 “balanced” northern part of the basin, where the competing effects of mortality (i.e., increases in
530 ground evaporation versus decreases in transpiration) are more balanced (Fig. 11). The level of
531 vegetation mortality played a less significant role in changing water yield in the southern “water-
532 limited” area. Vegetation mortality level determined the magnitudes of Live LAI, Total LAI,
533 transpiration, canopy evaporation, and ground evaporation in such a way that it governed the
534 direction of change in both ET and water yield. Thus, when vegetation mortality level was higher
535 than 40%, its effect of decreasing transpiration became the dominant process and its effect of
536 increasing soil evaporation became minor (Fig. 11 f&g; Guardiola-Claramonte et al. 2011).

537 Besides the precipitation threshold of at least 500 mm/year, Adams et al. (2012) also estimate
538 that when at least 20% of vegetation cover is removed, water yield can increase. According to
539 previous analysis (Sect 4.1), for a dry year, water yield increases when more than 40% of
540 vegetation is removed (Fig. 10a). Our model simulations indicate similar mortality thresholds
541 exist for driving water yield increases during the dry year, however, we did not find evidence
542 that such a threshold exists during wet years. These differences between dry and wet years



543 suggest that the effects of mortality on water yield depend on climate variability. Other studies
544 corroborate this finding by demonstrating that the relationship between mortality level and water
545 yield response is complicated and nonlinear (Moore and Wondzell 2005).

546 5.3 Role of long-term aridity index (PET/P)

547 Long-term aridity indices can be used to predict where water yield will decrease after
548 disturbance. We found that water yield always increased in a wet year, irrespective of the
549 climatic aridity index (Fig. 10a). For dry years, long-term aridity index became important in
550 driving the direction of water yield responses to beetle outbreak. In areas that are less water-
551 limited (balanced areas), the direction of water-yield responses to beetle outbreak in a dry year
552 was mixed and depended on mortality level. For water-limited areas, in a dry year, water yield
553 showed a more consistent decrease trend, and it was also less affected by mortality level. These
554 results agree with previous studies finding that water yield decreases largely happen in semiarid
555 areas (Guardiola-Claramonte et al. 2011; Biederman et al. 2014).

556 The decrease in water yield for water-limited area can be driven by increases in canopy
557 evaporation or transpiration, which were different in the hydrologically-balanced area (driven by
558 increase of ground evaporation). There, the increase in canopy evaporation was due to an
559 increase in total LAI which is a combined effect of delayed decay of dead foliage and fast
560 growth of residual and understory plants (Fig. 11d type D5, D7, D8 & D9; Fig. S5). The
561 surviving and understory plants in the water-limited area can also have higher transpiration rates
562 after mortality (Fig. 11d type D6 and Fig. 8). Similarly, in field studies, Tsamir et al. (2019)
563 found an increase in photosynthesis and transpiration after thinning in a semi-arid forest. These
564 findings illustrate that in addition to top-down climate variability, the long-term aridity index



565 (which also varies with bottom-up drivers such as vegetation and local topography) can be
566 another useful indicator of how water yield will respond to disturbances.

567 5.4 Uncertainties

568 While our findings revealed how topoclimatic gradients influenced water yield responses to
569 beetle infestation, some uncertainties remain. For one, we used uniform mortality levels for all
570 patches across the watershed rather than location and vegetation-specific mortality levels.
571 However, in reality beetles usually attack older trees first (Edburg et al. 2011). Thus,
572 incorporating a more mechanistic understanding of beetle attack patterns with our beetle effects
573 model could enable us to simulate more realistic outbreak scenarios moving forward. Another
574 source of uncertainty came from the model treatment of litter pools. In the current
575 implementation, we ignored the effects of litter on ground albedo and snowmelt (Lundquist et al.
576 2013), which could have an effect on rates of AET and PET and therefore our calculated long-
577 term aridity index. Also, because we focused on water yield responses during the first 15 years
578 after beetle outbreak, we may have missed some of the long-term effects (e.g., after the
579 ecosystem has begun to recover) on forest hydrology. Future research should integrate the short-
580 term and long-term effects and interactions among beetle outbreak, vegetation dynamics, and
581 hydrology. Since Trail Creek is either “balanced” or “water-limited” in terms of aridity, other
582 “energy-limited” regions could also be investigated.

583 **6 Conclusion**

584 We tested a coupled ecohydrologic and beetle effects model in a semi-arid basin in southern
585 Idaho to examine how watershed hydrology responds to beetle outbreak and how interannual
586 climatic variability, vegetation mortality, and long-term aridity influence these responses.
587 Simulation results indicate that each factor can play a discrete role in driving hydrological



588 processes (e.g., the direction and magnitude of changes in plant transpiration, canopy and soil
589 evaporation, soil and litter moisture, snow sublimation, etc.). These combined effects determine
590 the overall water budget and water yield of the basin. While interannual climate variability is the
591 key factor driving the direction of change in water yield, vegetation mortality levels and long-
592 term aridity modify water yield responses.

593 In dry years, the water yield of most sub-basins slightly decreased after beetle outbreak when
594 vegetation mortality level was lower than 40%; while during wet years in most sub-basins it
595 increased. Our results show that long-term aridity index is a reliable indicator of the water yield
596 decreases that occur during dry years due to the fact that there is a consistent decrease in water
597 yield in the most water-limited portion of the basin. Generally, the effects of vegetation mortality
598 on water yield during dry years is less uniform and depends on local, long-term aridity
599 conditions. During wet years, on the other hand, mortality typically causes increases in water
600 yield. This illustrates that together interannual climate variability and mortality can have a
601 stronger effect on the direction of water yield response in water-limited regions than interannual
602 climate variability alone. Future studies to predict water yield response to disturbance should
603 consider the interactions of these factors and capture the fluctuations of competing water fluxes
604 and storage change that control overall water budget and water yield.

605 Using our novel RHESSys-beetle effects modeling framework, we demonstrate that the direction
606 of hydrologic response is a function of multiple factors (e.g., interannual climate variability,
607 vegetation mortality level, and long-term aridity) and that these results do not necessarily *conflict*
608 with each other but are representative of different conditions. The mechanisms behind these
609 changes compete with each other resulting in a water yield increases or decreases (Fig. 1).

610 Contradictory findings in previous studies may result from differing mortality levels (disturbance



611 severity), or differences in aridity, and consequently, the emergent drivers that dominate water
612 yield responses differ. Disentangling these drivers is difficult or impossible using a purely
613 empirical approach where it can be challenging or cost-prohibitive to experiment under a broad
614 range of controlled conditions. Distributed process-based models on the other hand, provide a
615 useful tool for examining these dynamics.

616 Findings from this study can assist water supply stakeholders in risk management in beetle
617 outbreak locations. For example, during wet years, more attention might be focused on
618 “balanced” areas, i.e., wet regions, for flooding and erosion risks after beetle outbreaks since
619 these regions may experience large increase in runoff due to decreases in plant transpiration and
620 increases in soil moisture. During the dry years, attention might need to shift to “water-limited”
621 areas for managing wildfire risk since these regions will experience elevated ET and lower soil
622 and litter moisture. Because multiple factors interact to influence hydrological processes after
623 beetle outbreak, water and forests management must respond to spatial and temporal variations
624 in climate, aridity, and vegetation mortality levels.

625 **Code and data availability**

626 The coupled RHESSys model code is available online at:

627 https://github.com/renjianning/RHESSys/tree/historical_fire

628 The data used in this study are available at:

629 https://osf.io/tsu9z/?view_only=72bfa7b376ad40c59278312f49b03a69

630 **Author contributions**

631 JR, JA and JAH conceived of study. JR designed study with support from JA, JAH and EH. JR
632 and EH developed RHESSys code for coupling beetle effect model and parallelizing model runs



633 with help from JA, JAH, NT, ML, CK, and JTA. JR performed model simulations and developed
634 figures with help from all authors. ML and JTA generated downscaled meteorological data. JR
635 wrote manuscript with input from all authors.

636 **Competing interests**

637 The authors declare that they have no conflict of interest.

638 **Acknowledgments**

639 This project is supported by National Science Foundation of United States under award number
640 DMS-1520873.

641



642 References

- 643 Ackerly, David D. 2004. “Adaptation, Niche Conservatism, and Convergence: Comparative
644 Studies of Leaf Evolution in the California Chaparral.” *The American Naturalist* 163 (5):
645 654–71. <https://doi.org/10.1086/383062>.
- 646 Adams, Henry D., Charles H. Luce, David D. Breshears, Craig D. Allen, Markus Weiler, V.
647 Cody Hale, Alistair M. S. Smith, and Travis E. Huxman. 2012. “Ecohydrological
648 Consequences of Drought- and Infestation- Triggered Tree Die-off: Insights and
649 Hypotheses.” *Ecohydrology* 5 (2): 145–59. <https://doi.org/10.1002/eco.233>.
- 650 Anderegg, William R. L., Jeffrey M. Kane, and Leander D. L. Anderegg. 2013. “Consequences
651 of Widespread Tree Mortality Triggered by Drought and Temperature Stress.” *Nature
652 Climate Change* 3 (1): 30–36. <https://doi.org/10.1038/nclimate1635>.
- 653 Baret, F., A. Olioso, J. L. Luciani, J. F. Hanocq, and J. C. Monterrot. 1989. “Estimation à partir
654 de mesures de réflectance spectrale du rayonnement photosynthétiquement actif absorbé
655 par une culture de blé.” *Agronomie* 9 (9): 885–95. <https://doi.org/10.1051/agro:19890906>.
- 656 Bart, Ryan R., Christina L. Tague, and Max A. Moritz. 2016. “Effect of Tree-to-Shrub Type
657 Conversion in Lower Montane Forests of the Sierra Nevada (USA) on Streamflow.”
658 Edited by Julia A. Jones. *PLOS ONE* 11 (8): e0161805.
659 <https://doi.org/10.1371/journal.pone.0161805>.
- 660 Bennett, Katrina E., Theodore J. Bohn, Kurt Solander, Nathan G. McDowell, Chonggang Xu,
661 Enrique Vivoni, and Richard S. Middleton. 2018. “Climate-Driven Disturbances in the
662 San Juan River Sub-Basin of the Colorado River.” *Hydrology and Earth System Sciences*
663 22 (1): 709–25. <https://doi.org/10.5194/hess-22-709-2018>.
- 664 Bentz, Barbara J., Jacques Régnière, Christopher J. Fettig, E. Matthew Hansen, Jane L. Hayes,
665 Jeffrey A. Hicke, Rick G. Kelsey, Jose F. Negrón, and Steven J. Seybold. 2010. “Climate
666 Change and Bark Beetles of the Western United States and Canada: Direct and Indirect
667 Effects.” *BioScience* 60 (8): 602–13. <https://doi.org/10.1525/bio.2010.60.8.6>.
- 668 BERNER, L. T., B. E. LAW, A. J. MEDDENS, and J. A. HICKE. 2017. “Tree Mortality from
669 Fires and Bark Beetles at 1-Km Resolution, Western USA, 2003-2012.” Collection. Tree
670 Mortality from Fires and Bark Beetles at 1-Km Resolution, Western USA, 2003-2012.
671 2017. <https://doi.org/10.3334/ornl daac/1512>.
- 672 Berner, Logan T., and Beverly E. Law. 2016. “Plant Traits, Productivity, Biomass and Soil
673 Properties from Forest Sites in the Pacific Northwest, 1999–2014.” *Scientific Data* 3 (1):
674 1–14. <https://doi.org/10.1038/sdata.2016.2>.
- 675 Bethlahmy, Nedavia. 1974. “More Streamflow after a Bark Beetle Epidemic.” *Journal of
676 Hydrology* 23 (3): 185–89. [https://doi.org/10.1016/0022-1694\(74\)90001-8](https://doi.org/10.1016/0022-1694(74)90001-8).
- 677 Biederman, J. A., A. A. Harpold, D. J. Gochis, B. E. Ewers, D. E. Reed, S. A. Papuga, and P. D.
678 Brooks. 2014. “Increased Evaporation Following Widespread Tree Mortality Limits
679 Streamflow Response.” *Water Resources Research* 50 (7): 5395–5409.
680 <https://doi.org/10.1002/2013WR014994>.
- 681 Buhidar, Balthasar. 2002. “The Big Wood River Watershed Management Plan.”
682 [https://www.deq.idaho.gov/media/450316-
683 _water_data_reports_surface_water_tm dls_big_wood_river_big_wood_entire.pdf](https://www.deq.idaho.gov/media/450316-_water_data_reports_surface_water_tm dls_big_wood_river_big_wood_entire.pdf).
- 684 Buma, Brian, and Ben Livneh. 2017. “Key Landscape and Biotic Indicators of Watersheds
685 Sensitivity to Forest Disturbance Identified Using Remote Sensing and Historical



- 686 Hydrography Data.” *Environmental Research Letters* 12 (7): 074028.
687 <https://doi.org/10.1088/1748-9326/aa7091>.
- 688 Chaney, Nathaniel W., Eric F. Wood, Alexander B. McBratney, Jonathan W. Hempel, Travis W.
689 Nauman, Colby W. Brungard, and Nathan P. Odgers. 2016. “POLARIS: A 30-Meter
690 Probabilistic Soil Series Map of the Contiguous United States.” *Geoderma* 274 (July):
691 54–67. <https://doi.org/10.1016/j.geoderma.2016.03.025>.
- 692 Chen, Fei, Guo Zhang, Michael Barlage, Ying Zhang, Jeffrey A. Hicke, Arjan Meddens,
693 Guangsheng Zhou, William J. Massman, and John Frank. 2014. “An Observational and
694 Modeling Study of Impacts of Bark Beetle–Caused Tree Mortality on Surface Energy and
695 Hydrological Cycles.” *Journal of Hydrometeorology* 16 (2): 744–61.
696 <https://doi.org/10.1175/JHM-D-14-0059.1>.
- 697 Daly, Christopher, Ronald P. Neilson, and Donald L. Phillips. 1994. “A Statistical-Topographic
698 Model for Mapping Climatological Precipitation over Mountainous Terrain.” *Journal of*
699 *Applied Meteorology* 33 (2): 140–58. [https://doi.org/10.1175/1520-0450\(1994\)033<0140:ASTMFM>2.0.CO;2](https://doi.org/10.1175/1520-0450(1994)033<0140:ASTMFM>2.0.CO;2).
- 700
701 Dickinson, Robert E., Muhammad Shaikh, Ross Bryant, and Lisa Graumlich. 1998. “Interactive
702 Canopies for a Climate Model.” *Journal of Climate* 11 (11): 2823–36.
703 [https://doi.org/10.1175/1520-0442\(1998\)011<2823:ICFACM>2.0.CO;2](https://doi.org/10.1175/1520-0442(1998)011<2823:ICFACM>2.0.CO;2).
- 704 Edburg, Steven L., Jeffrey A. Hicke, Paul D. Brooks, Elise G. Pendall, Brent E. Ewers, Urszula
705 Norton, David Gochis, Ethan D. Gutmann, and Arjan JH Meddens. 2012. “Cascading
706 Impacts of Bark Beetle-Caused Tree Mortality on Coupled Biogeophysical and
707 Biogeochemical Processes.” *Frontiers in Ecology and the Environment* 10 (8): 416–24.
708 <https://doi.org/10.1890/110173>.
- 709 Edburg, Steven L., Jeffrey A. Hicke, David M. Lawrence, and Peter E. Thornton. 2011.
710 “Simulating Coupled Carbon and Nitrogen Dynamics Following Mountain Pine Beetle
711 Outbreaks in the Western United States.” *Journal of Geophysical Research:*
712 *Biogeosciences* 116 (G4): G04033. <https://doi.org/10.1029/2011JG001786>.
- 713 Fan, Y., M. Clark, D. M. Lawrence, S. Swenson, L. E. Band, S. L. Brantley, P. D. Brooks, et al.
714 2019. “Hillslope Hydrology in Global Change Research and Earth System Modeling.”
715 *Water Resources Research* 0 (0). <https://doi.org/10.1029/2018WR023903>.
- 716 Farquhar, G. D., and S. von Caemmerer. 1982. “Modelling of Photosynthetic Response to
717 Environmental Conditions.” In *Physiological Plant Ecology II: Water Relations and*
718 *Carbon Assimilation*, edited by O. L. Lange, P. S. Nobel, C. B. Osmond, and H. Ziegler,
719 549–87. Encyclopedia of Plant Physiology. Berlin, Heidelberg: Springer.
720 https://doi.org/10.1007/978-3-642-68150-9_17.
- 721 Frenzel, Steven A. 1989. “Water Resources of the Upper Big Wood River Basin, Idaho.” US
722 Geological Survey. <https://idwr.idaho.gov/files/legal/CMR50/CMR50-1989-Water-Resources-of-the-Upper-Big-Wood-River-Basin-Idaho.pdf>.
- 723
724 Fyfe, John C., Chris Derksen, Lawrence Mudryk, Gregory M. Flato, Benjamin D. Santer, Neil C.
725 Swart, Noah P. Molotch, et al. 2017. “Large Near-Term Projected Snowpack Loss over
726 the Western United States.” *Nature Communications* 8 (1): 14996.
727 <https://doi.org/10.1038/ncomms14996>.
- 728 Garcia, E. S., and C. L. Tague. 2015. “Subsurface Storage Capacity Influences Climate–
729 Evapotranspiration Interactions in Three Western United States Catchments.” *Hydrology*
730 *and Earth System Sciences* 19 (12): 4845–58. <https://doi.org/10.5194/hess-19-4845-2015>.



- 731 Goeking, Sara A., and David G. Tarboton. 2020. “Forests and Water Yield: A Synthesis of
732 Disturbance Effects on Streamflow and Snowpack in Western Coniferous Forests.”
733 *Journal of Forestry* 118 (2): 172–92. <https://doi.org/10.1093/jofore/fvz069>.
- 734 Guardiola-Claramonte, M., Peter A. Troch, David D. Breshears, Travis E. Huxman, Matthew B.
735 Switanek, Matej Durcik, and Neil S. Cobb. 2011. “Decreased Streamflow in Semi-Arid
736 Basins Following Drought-Induced Tree Die-off: A Counter-Intuitive and Indirect
737 Climate Impact on Hydrology.” *Journal of Hydrology* 406 (3): 225–33.
738 <https://doi.org/10.1016/j.jhydrol.2011.06.017>.
- 739 Hanan, Erin J., Carla M. D’Antonio, Dar A. Roberts, and Joshua P. Schimel. 2016. “Factors
740 Regulating Nitrogen Retention During the Early Stages of Recovery from Fire in Coastal
741 Chaparral Ecosystems.” *Ecosystems* 19 (5): 910–26. <https://doi.org/10.1007/s10021-016-9975-0>.
- 742
743 Hanan, Erin J., Christina Tague, Janet Choate, Mingliang Liu, Crystal Kolden, and Jennifer
744 Adam. 2018. “Accounting for Disturbance History in Models: Using Remote Sensing to
745 Constrain Carbon and Nitrogen Pool Spin-Up.” *Ecological Applications: A Publication
746 of the Ecological Society of America* 28 (5): 1197–1214.
747 <https://doi.org/10.1002/eap.1718>.
- 748 Hanan, Erin J., Christina (Naomi) Tague, and Joshua P. Schimel. 2017. “Nitrogen Cycling and
749 Export in California Chaparral: The Role of Climate in Shaping Ecosystem Responses to
750 Fire.” *Ecological Monographs* 87 (1): 76–90. <https://doi.org/10.1002/ecm.1234>.
- 751 Hicke, Jeffrey A., Morris C. Johnson, Jane L. Hayes, and Haiganoush K. Preisler. 2012. “Effects
752 of Bark Beetle-Caused Tree Mortality on Wildfire.” *Forest Ecology and Management*
753 271 (May): 81–90. <https://doi.org/10.1016/j.foreco.2012.02.005>.
- 754 Homer, Collin G., Jon Dewitz, Limin Yang, Suming Jin, Patrick Danielson, George Z. Xian,
755 John Coulston, Nathaniel Herold, James Wickham, and Kevin Megown. 2015.
756 “Completion of the 2011 National Land Cover Database for the Conterminous United
757 States – Representing a Decade of Land Cover Change Information.” *Photogrammetric
758 Engineering and Remote Sensing* 81: 345354.
- 759 Hubbart, Jason A. 2007. “Timber Harvest Impacts on Water Yield in the Continental/Maritime
760 Hydroclimatic Region of the United States,” 12.
- 761 Law, B. E., O. J. Sun, J. Campbell, S. Van Tuyl, and P. E. Thornton. 2003. “Changes in Carbon
762 Storage and Fluxes in a Chronosequence of Ponderosa Pine.” *Global Change Biology* 9
763 (4): 510–24. <https://doi.org/10.1046/j.1365-2486.2003.00624.x>.
- 764 Lawrence, David M., Keith W. Oleson, Mark G. Flanner, Peter E. Thornton, Sean C. Swenson,
765 Peter J. Lawrence, Xubin Zeng, et al. 2011. “Parameterization Improvements and
766 Functional and Structural Advances in Version 4 of the Community Land Model.”
767 *Journal of Advances in Modeling Earth Systems* 3 (1).
768 <https://doi.org/10.1029/2011MS00045>.
- 769 Lin, Laurence, Lawrence E. Band, James M. Vose, Taehee Hwang, Chelcy Ford Miniati, and
770 Paul V. Bolstad. 2019. “Ecosystem Processes at the Watershed Scale: Influence of
771 Flowpath Patterns of Canopy Ecophysiology on Emergent Catchment Water and Carbon
772 Cycling.” *Ecohydrology* 0 (0): e2093. <https://doi.org/10.1002/eco.2093>.
- 773 Livneh, Ben, Jeffrey S. Deems, Brian Buma, Joseph J. Barsugli, Dominik Schneider, Noah P.
774 Molotch, K. Wolter, and Carol A. Wessman. 2015. “Catchment Response to Bark Beetle
775 Outbreak and Dust-on-Snow in the Colorado Rocky Mountains.” *Journal of Hydrology*
776 523 (April): 196–210. <https://doi.org/10.1016/j.jhydrol.2015.01.039>.



- 777 Lundquist, Jessica D., Susan E. Dickerson-Lange, James A. Lutz, and Nicoleta C. Cristea. 2013.
778 “Lower Forest Density Enhances Snow Retention in Regions with Warmer Winters: A
779 Global Framework Developed from Plot-Scale Observations and Modeling.” *Water*
780 *Resources Research* 49 (10): 6356–70. <https://doi.org/10.1002/wrcr.20504>.
- 781 Lundquist, Jessica D., Paul J. Neiman, Brooks Martner, Allen B. White, Daniel J. Gottas, and F.
782 Martin Ralph. 2008. “Rain versus Snow in the Sierra Nevada, California: Comparing
783 Doppler Profiling Radar and Surface Observations of Melting Level.” *Journal of*
784 *Hydrometeorology* 9 (2): 194–211. <https://doi.org/10.1175/2007JHM853.1>.
- 785 McVicar, Tim R., Michael L. Roderick, Randall J. Donohue, Ling Tao Li, Thomas G. Van Niel,
786 Axel Thomas, Jürgen Grieser, et al. 2012. “Global Review and Synthesis of Trends in
787 Observed Terrestrial Near-Surface Wind Speeds: Implications for Evaporation.” *Journal*
788 *of Hydrology* 416–417 (January): 182–205. <https://doi.org/10.1016/j.jhydrol.2011.10.024>.
- 789 Meddens, Arjan, Jeffrey A Hicke, and Charles A Ferguson. 2012. “Spatiotemporal Patterns of
790 Observed Bark Beetle-Caused Tree Mortality in British Columbia and the Western
791 United States.” *Ecological Applications : A Publication of the Ecological Society of*
792 *America* 22 (October): 1876–91. <https://doi.org/10.2307/41723101>.
- 793 Mikkelsen, K. M., R. M. Maxwell, I. Ferguson, J. D. Stednick, J. E. McCray, and J. O. Sharp.
794 2013. “Mountain Pine Beetle Infestation Impacts: Modeling Water and Energy Budgets
795 at the Hill-Slope Scale.” *Ecohydrology* 6 (1): 64–72. <https://doi.org/10.1002/eco.278>.
- 796 Mitchell, Kenneth E., Dag Lohmann, Paul R. Houser, Eric F. Wood, John C. Schaake, Alan
797 Robock, Brian A. Cosgrove, et al. 2004. “The Multi-Institution North American Land
798 Data Assimilation System (NLDAS): Utilizing Multiple GCIP Products and Partners in a
799 Continental Distributed Hydrological Modeling System.” In .
800 <https://doi.org/10.1029/2003JD003823>.
- 801 Monteith, J. L. 1965. “Evaporation and Environment.” *Symposia of the Society for Experimental*
802 *Biology* 19: 205–34.
- 803 Montesi, James, Kelly Elder, R. A. Schmidt, and Robert E. Davis. 2004. “Sublimation of
804 Intercepted Snow within a Subalpine Forest Canopy at Two Elevations.” *Journal of*
805 *Hydrometeorology* 5 (5): 763–73. [https://doi.org/10.1175/1525-7541\(2004\)005<0763:SOISWA>2.0.CO;2](https://doi.org/10.1175/1525-7541(2004)005<0763:SOISWA>2.0.CO;2).
- 806
- 807 Moore, R Dan, and S M Wondzell. 2005. “PHYSICAL HYDROLOGY AND THE EFFECTS
808 OF FOREST HARVESTING IN THE PACIFIC NORTHWEST: A REVIEW,” 22.
- 809 Morillas, L., R. E. Pangle, G. E. Maurer, W. T. Pockman, N. McDowell, C.-W. Huang, D. J.
810 Krofcheck, et al. 2017. “Tree Mortality Decreases Water Availability and Ecosystem
811 Resilience to Drought in Piñon-Juniper Woodlands in the Southwestern U.S.” *Journal of*
812 *Geophysical Research: Biogeosciences* 122 (12): 3343–61.
813 <https://doi.org/10.1002/2017JG004095>.
- 814 Mu, Qiaozhen, Faith Ann Heinsch, Maosheng Zhao, and Steven W. Running. 2007.
815 “Development of a Global Evapotranspiration Algorithm Based on MODIS and Global
816 Meteorology Data.” *Remote Sensing of Environment* 111 (4): 519–36.
817 <https://doi.org/10.1016/j.rse.2007.04.015>.
- 818 Mu, Qiaozhen, Maosheng Zhao, and Steven W. Running. 2011. “Improvements to a MODIS
819 Global Terrestrial Evapotranspiration Algorithm.” *Remote Sensing of Environment* 115
820 (8): 1781–1800. <https://doi.org/10.1016/j.rse.2011.02.019>.



- 821 Nash, J. E., and J. V. Sutcliffe. 1970. “River Flow Forecasting through Conceptual Models Part I
822 — A Discussion of Principles.” *Journal of Hydrology* 10 (3): 282–90.
823 [https://doi.org/10.1016/0022-1694\(70\)90255-6](https://doi.org/10.1016/0022-1694(70)90255-6).
- 824 NRCS. n.d. “SNOTEL.” https://www.wcc.nrcs.usda.gov/about/mon_automate.html.
- 825 Paine, T. D., K. F. Raffa, and T. C. Harrington. 1997. “Interactions Among Scolytid Bark
826 Beetles, Their Associated Fungi, and Live Host Conifers.” *Annual Review of Entomology*
827 42 (1): 179–206. <https://doi.org/10.1146/annurev.ento.42.1.179>.
- 828 Parton, W. J., A. R. Mosier, D. S. Ojima, D. W. Valentine, D. S. Schimel, K. Weier, and A. E.
829 Kulmala. 1996. “Generalized Model for N₂ and N₂O Production from Nitrification and
830 Denitrification.” *Global Biogeochemical Cycles* 10 (3): 401–12.
831 <https://doi.org/10.1029/96GB01455>.
- 832 Penn, Colin A., Lindsay A. Bearup, Reed M. Maxwell, and David W. Clow. 2016. “Numerical
833 Experiments to Explain Multiscale Hydrological Responses to Mountain Pine Beetle Tree
834 Mortality in a Headwater Watershed.” *Water Resources Research* 52 (4): 3143–61.
835 <https://doi.org/10.1002/2015WR018300>.
- 836 Perry, Timothy D., and Julia A. Jones. 2017. “Summer Streamflow Deficits from Regenerating
837 Douglas-Fir Forest in the Pacific Northwest, USA: Summer Streamflow Deficits from
838 Regenerating Douglas-Fir Forest.” *Ecohydrology* 10 (2): e1790.
839 <https://doi.org/10.1002/eco.1790>.
- 840 Pomeroy, John, Xing Fang, and Chad Ellis. 2012. “Sensitivity of Snowmelt Hydrology in
841 Marmot Creek, Alberta, to Forest Cover Disturbance: SENSITIVITY OF SNOWMELT
842 HYDROLOGY TO FOREST DISTURBANCE.” *Hydrological Processes* 26 (12): 1891–
843 1904. <https://doi.org/10.1002/hyp.9248>.
- 844 Potts, Donald F. 1984. “Hydrologic Impacts of a Large-Scale Mountain Pine Beetle
845 (*Dendroctonus Ponderosae* Hopkins) Epidemic1.” *JAWRA Journal of the American*
846 *Water Resources Association* 20 (3): 373–77. [https://doi.org/10.1111/j.1752-
847 1688.1984.tb04719.x](https://doi.org/10.1111/j.1752-1688.1984.tb04719.x).
- 848 Robles, Marcos D., Robert M. Marshall, Frances O’Donnell, Edward B. Smith, Jeanmarie A.
849 Haney, and David F. Gori. 2014. “Effects of Climate Variability and Accelerated Forest
850 Thinning on Watershed-Scale Runoff in Southwestern USA Ponderosa Pine Forests.”
851 *PLOS ONE* 9 (10): e111092. <https://doi.org/10.1371/journal.pone.0111092>.
- 852 Ryan, Michael G. 1991. “Effects of Climate Change on Plant Respiration.” *Ecological*
853 *Applications* 1 (2): 157–67. <https://doi.org/10.2307/1941808>.
- 854 Searcy, James Kincheon. 1959. “Flow-Duration Curves.” Report 1542A. Water Supply Paper.
855 USGS Publications Warehouse. <https://doi.org/10.3133/wsp1542A>.
- 856 Sexstone, Graham A., David W. Clow, Steven R. Fassnacht, Glen E. Liston, Christopher A.
857 Hiemstra, John F. Knowles, and Colin A. Penn. 2018. “Snow Sublimation in Mountain
858 Environments and Its Sensitivity to Forest Disturbance and Climate Warming.” *Water*
859 *Resources Research* 54 (2): 1191–1211. <https://doi.org/10.1002/2017WR021172>.
- 860 Skinner, Kenneth D. 2013. “Post-Fire Debris-Flow Hazard Assessment of the Area Burned by
861 the 2013 Beaver Creek Fire near Hailey, Central Idaho.” USGS Numbered Series 2013–
862 1273. Open-File Report. Reston, VA: U.S. Geological Survey.
863 <http://pubs.er.usgs.gov/publication/ofr20131273>.
- 864 Sliniski, Kimberly M., Terri S. Hogue, Aaron T. Porter, and John E. McCray. 2016. “Recent Bark
865 Beetle Outbreaks Have Little Impact on Streamflow in the Western United States.”



- 866 *Environmental Research Letters* 11 (7): 074010. <https://doi.org/10.1088/1748-9326/11/7/074010>.
- 867
- 868 Smith, Frederick W., D. Arthur Sampson, and James N. Long. 1991. “Comparison of Leaf Area
- 869 Index Estimates from Tree Allometrics and Measured Light Interception.” *Forest Science*
- 870 37 (6): 1682–88. <https://doi.org/10.1093/forestscience/37.6.1682>.
- 871 Smith, Rex Onis. 1960. “Geohydrologic Evaluation of Streamflow Records in the Big Wood
- 872 River Basin, Idaho.” USGS Numbered Series 1479. Water Supply Paper. U.S. Govt.
- 873 Print. Off.,. <http://pubs.er.usgs.gov/publication/wsp1479>.
- 874 Son, Kyongho, and Christina Tague. 2019. “Hydrologic Responses to Climate Warming for a
- 875 Snow-Dominated Watershed and a Transient Snow Watershed in the California Sierra.”
- 876 *Ecohydrology* 12 (1): e2053. <https://doi.org/10.1002/eco.2053>.
- 877 Sun, Ning, Mark Wigmosta, Tian Zhou, Jessica Lundquist, Susan Dickerson-Lange, and
- 878 Nicoleta Cristea. 2018. “Evaluating the Functionality and Streamflow Impacts of
- 879 Explicitly Modelling Forest–Snow Interactions and Canopy Gaps in a Distributed
- 880 Hydrologic Model.” *Hydrological Processes* 32 (13): 2128–40.
- 881 <https://doi.org/10.1002/hyp.13150>.
- 882 Tague, C. L., and L. E. Band. 2004. “RHESSys: Regional Hydro-Ecologic Simulation System—
- 883 An Object-Oriented Approach to Spatially Distributed Modeling of Carbon, Water, and
- 884 Nutrient Cycling.” *Earth Interactions* 8 (19): 1–42. [https://doi.org/10.1175/1087-3562\(2004\)8<1:RRHSSO>2.0.CO;2](https://doi.org/10.1175/1087-3562(2004)8<1:RRHSSO>2.0.CO;2).
- 885
- 886 Tague, Christina L., Max Moritz, and Erin Hanan. 2019. “The Changing Water Cycle: The Eco-
- 887 Hydrologic Impacts of Forest Density Reduction in Mediterranean (Seasonally Dry)
- 888 Regions.” *Wiley Interdisciplinary Reviews: Water* 0 (0): e1350.
- 889 <https://doi.org/10.1002/wat2.1350>.
- 890 Tsamir, Mor, Sagi Gottlieb, Yakir Preisler, Eyal Rotenberg, Fyodor Tatarinov, Dan Yakir,
- 891 Christina Tague, and Tamir Klein. 2019. “Stand Density Effects on Carbon and Water
- 892 Fluxes in a Semi-Arid Forest, from Leaf to Stand-Scale.” *Forest Ecology and*
- 893 *Management* 453 (December): 117573. <https://doi.org/10.1016/j.foreco.2019.117573>.
- 894 White, Joseph D., and Steven W. Running. 1994. “Testing Scale Dependent Assumptions in
- 895 Regional Ecosystem Simulations.” *Journal of Vegetation Science* 5 (5): 687–702.
- 896 <https://doi.org/10.2307/3235883>.
- 897 White, Michael A., Peter E. Thornton, Steven W. Running, and Ramakrishna R. Nemani. 2000.
- 898 “Parameterization and Sensitivity Analysis of the BIOME–BGC Terrestrial Ecosystem
- 899 Model: Net Primary Production Controls.” *Earth Interactions* 4 (3): 1–85.
- 900 [https://doi.org/10.1175/1087-3562\(2000\)004<0003:PASAOT>2.0.CO;2](https://doi.org/10.1175/1087-3562(2000)004<0003:PASAOT>2.0.CO;2).
- 901 Wine, Michael L, Daniel Cadol, and Oleg Makhnin. 2018. “In Ecoregions across Western USA
- 902 Streamflow Increases during Post-Wildfire Recovery.” *Environmental Research Letters*
- 903 13 (1): 014010. <https://doi.org/10.1088/1748-9326/aa9c5a>.
- 904 Winkler, Rita, Sarah Boon, Barbara Zimonick, and Dave Spittlehouse. 2014. “Snow
- 905 Accumulation and Ablation Response to Changes in Forest Structure and Snow Surface
- 906 Albedo after Attack by Mountain Pine Beetle.” *Hydrological Processes* 28 (2): 197–209.
- 907 <https://doi.org/10.1002/hyp.9574>.
- 908 Zhang, Ke, John S. Kimball, Qiaozhen Mu, Lucas A. Jones, Scott J. Goetz, and Steven W.
- 909 Running. 2009. “Satellite Based Analysis of Northern ET Trends and Associated
- 910 Changes in the Regional Water Balance from 1983 to 2005.” *Journal of Hydrology* 379
- 911 (1): 92–110. <https://doi.org/10.1016/j.jhydrol.2009.09.047>.



912 Zhao, Maosheng, Steven W. Running, and Ramakrishna R. Nemani. 2006. "Sensitivity of
913 Moderate Resolution Imaging Spectroradiometer (MODIS) Terrestrial Primary
914 Production to the Accuracy of Meteorological Reanalyses." *Journal of Geophysical*
915 *Research: Biogeosciences* 111 (G1). <https://doi.org/10.1029/2004JG000004>.

916

917

918

919 *Table 1. Classification of aridity index.*

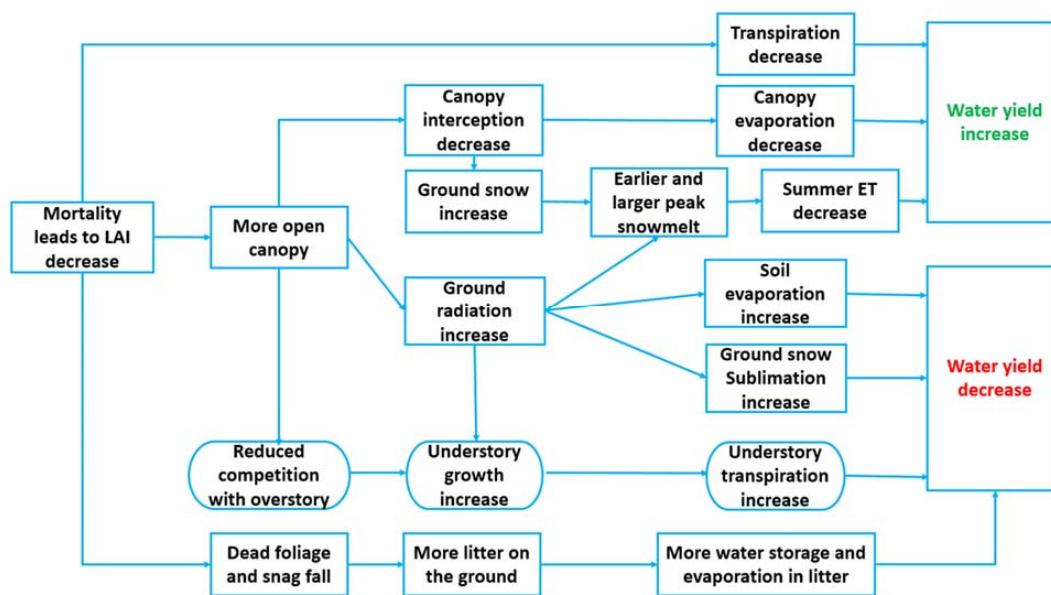
920

Aridity Index (i.e. PET/P)	Type
> 2	Water - limited
0.8 - 2	Balanced
< 0.8	Energy - limited

921

922

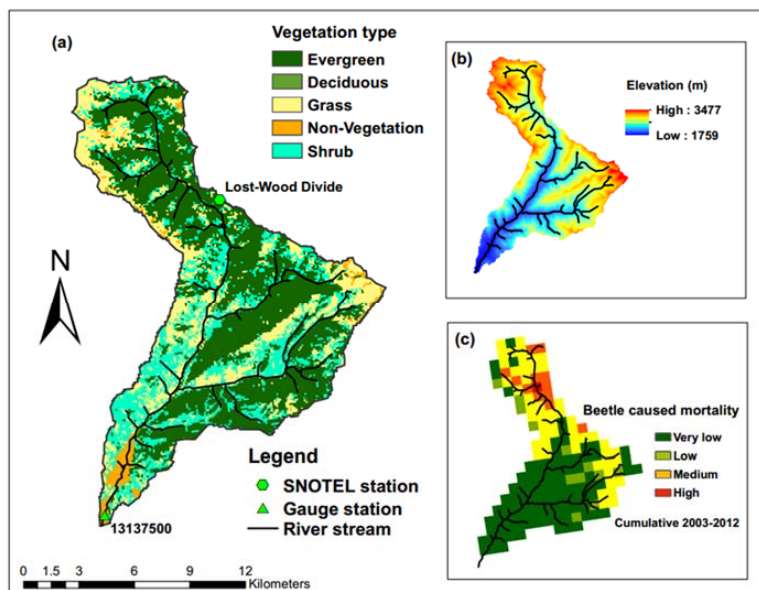
923



924

925 *Figure 1. Mechanism of water yield responses to beetle-caused mortality during the red and*
926 *gray phases (0 – 10 years after beetle outbreak), semicircle boxes represent understory*
927 *responses and square boxes represent overstory responses.*

928

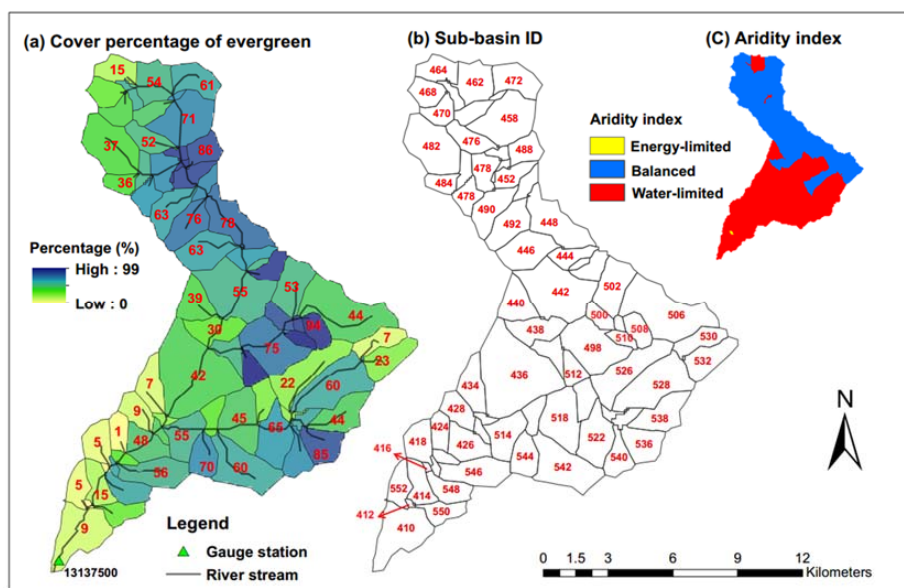


929

930 *Figure 2. Land cover, elevation, and tree mortality for Trail Creek. (a) is the land cover map*
931 *with the main vegetation type, (b) is the elevation gradient, and (c) is the severity of beetle*
932 *caused tree mortality (during the period 2003-2012 Meddens et al. (2012)). Note that, for our*
933 *modeling experiments, we prescribe beetle outbreak uniformly across evergreen patches instead*
934 *of using historical beetle outbreak data.*

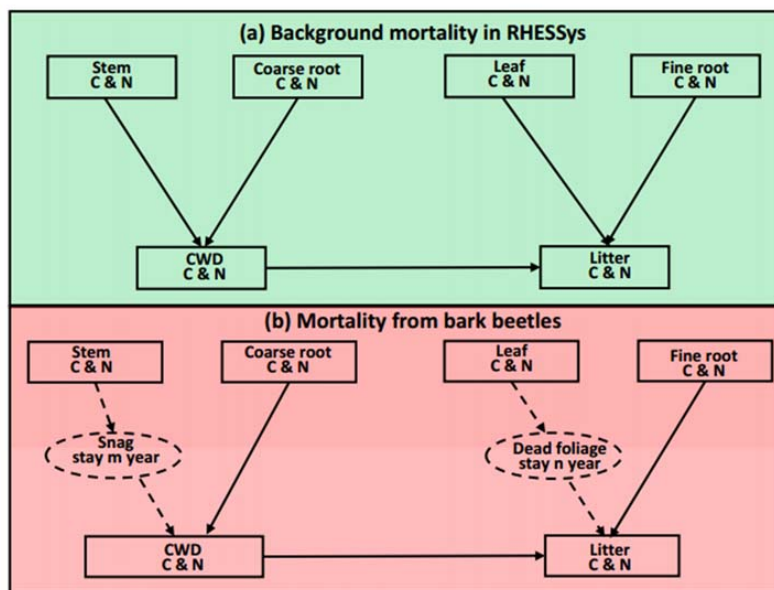
935

936



937

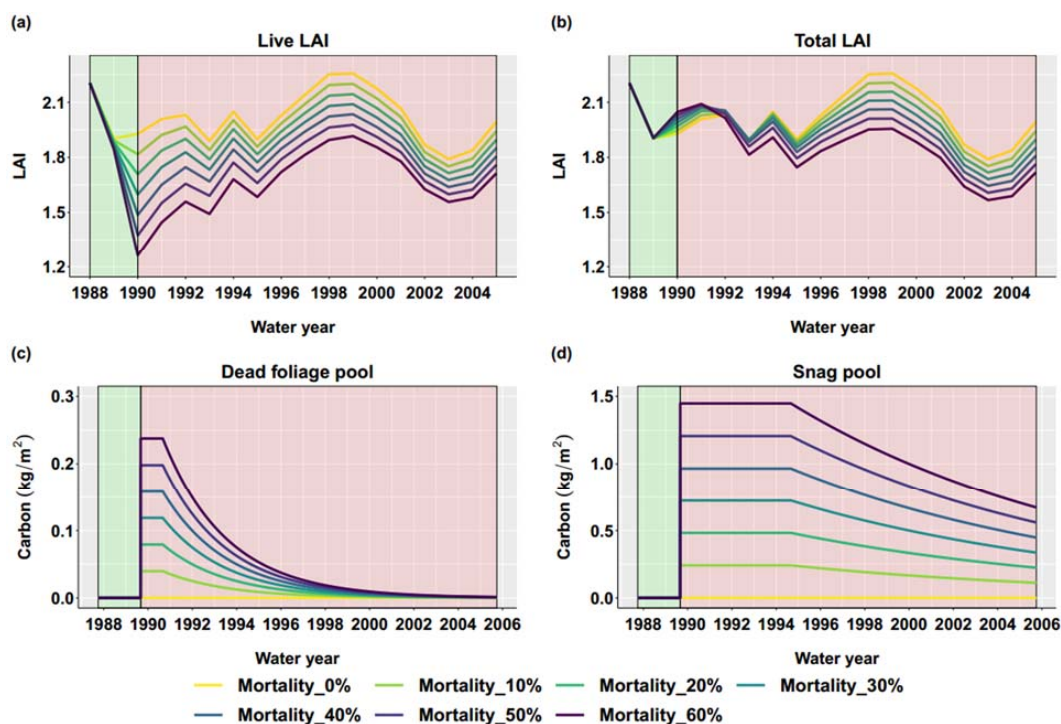
938 *Figure 3. Trail creek evergreen forest cover percentage for each sub-basin, sub-basin ID, and*
939 *long-term aridity index. Aridity index is defined as annual mean potential evapotranspiration*
940 *(PET) / precipitation (P) from 38 years of data (see Sect 3.4), $PET/P > 2$ is water-limited, PET/P*
941 *< 0.8 is energy-limited, PET/P between 0.8 and 2 is balanced. Recall that only evergreen forest*
942 *trees are attacked during beetle outbreaks.*
943



944

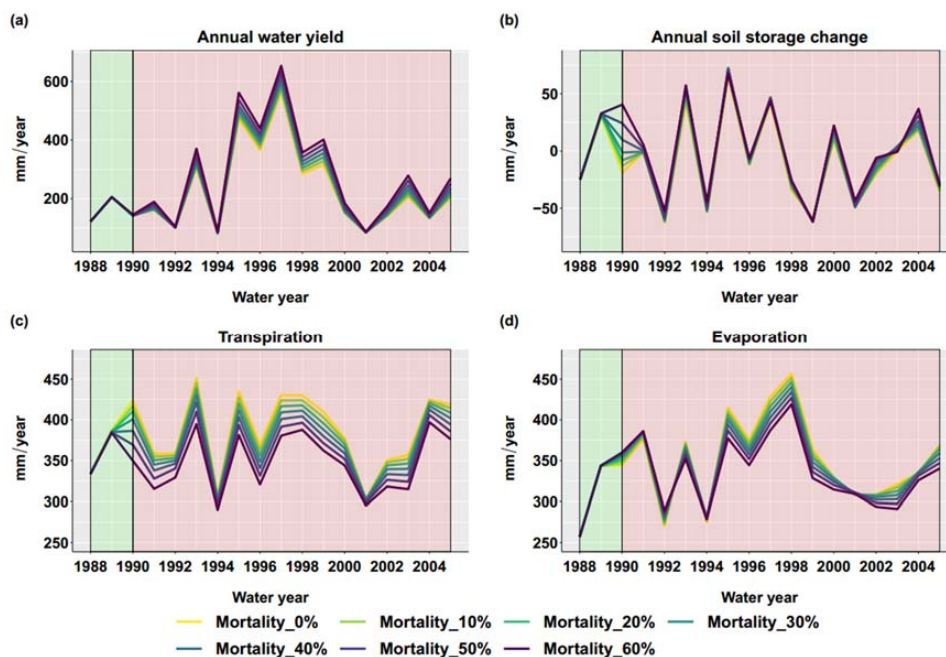
945 *Figure 4. Conceptual framework of the beetle effect model.*

946 *(a) Normal background mortality routine in RHESSys before beetle outbreak. (b) Mortality from*
947 *bark beetles. We add snag (standing dead trees) and dead foliage (needles still on dead trees)*
948 *pools, shown in the dashed circle. After a beetle outbreak, carbon (C) and Nitrogen (N) move*
949 *from stems to snag pools (black dashed arrow). After staying in the snag pool for m years, C and*
950 *N move from snag to coarse wood debris pools (CWD) with an exponential decay rate to*
951 *represent the snag fall (gray dashed arrow). It is a similar process for leaf C and N, which move*
952 *from leaf to dead foliage to litter pools (black dotted arrow). Furthermore, C and N in the CWD*
953 *and fine root pools move to the litter pool immediately after outbreak (solid black and gray*
954 *arrows). Figure modified from Edburg et al. (2012).*
955



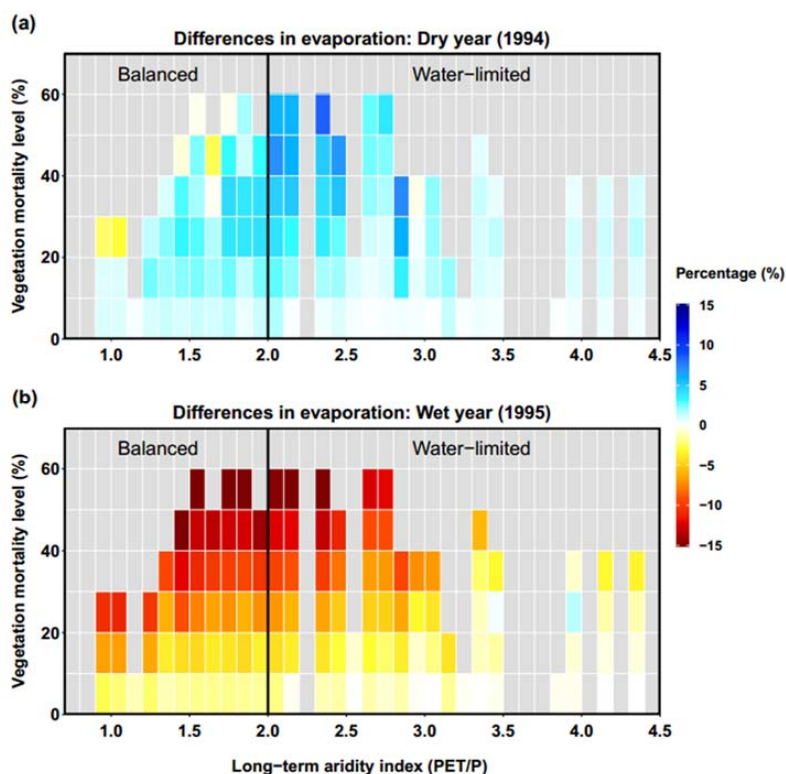
956

957 *Figure 5. Basin-scale vegetation responses after beetle outbreak for different evergreen*
958 *mortality level. (a) Annual live leaf area index (Live LAI), (b) Annual total LAI (LAI calculated*
959 *including dead foliage pool), (c) Daily dead foliage pool, and (d) Daily snag pool after outbreak.*
960 *The green background color is the period before beetle outbreak, and the red background color*
961 *is after the beetle outbreak.*
962



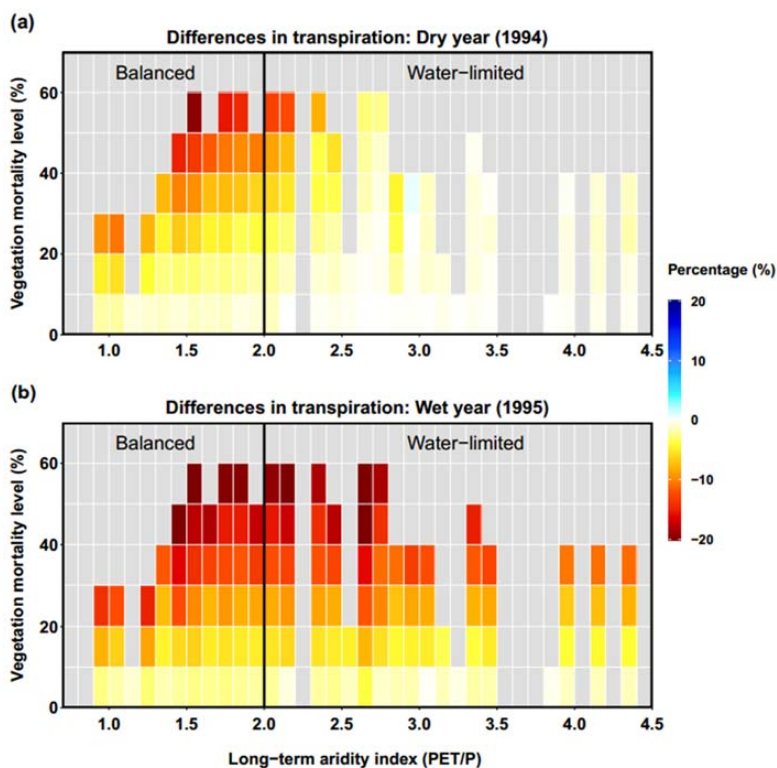
963

964 *Figure 6. Basin-scale annual sum of hydrologic fluxes responses after beetle outbreak (1989) for*
965 *different evergreen mortality levels. (a) Annual water yield calculated as annual sum of basin*
966 *streamflow, and (b) annual soil water storage change calculated as water year soil water*
967 *storage at the end of water year minus soil water storage at the beginning of water year. (c)*
968 *Transpiration is the annual sum of transpiration for both overstory and understory. (d)*
969 *Evaporation is calculated as the annual sum of canopy evaporation, ground evaporation, and*
970 *snow sublimation.*
971



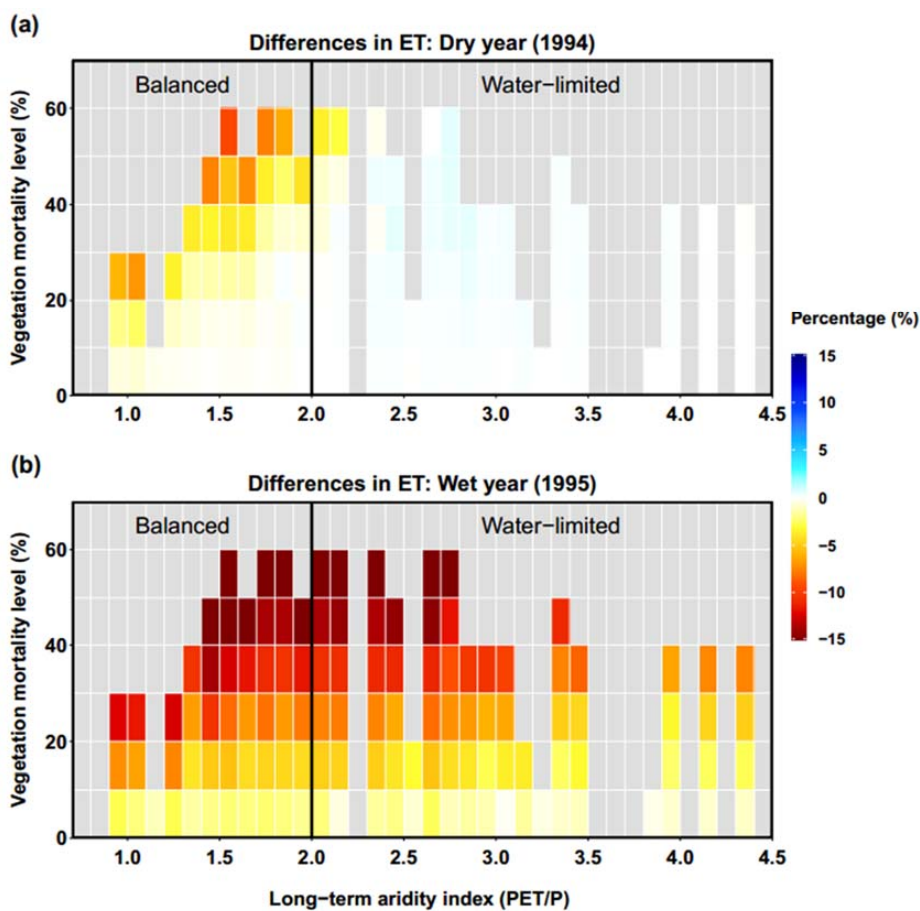
972

973 *Figure 7. Relationship among long-term aridity, vegetation mortality level, and differences in*
974 *evaporation for a dry year (1994, a) and wet year (1995, b). Differences are calculated as the*
975 *normalized differences (%) of evaporation between each evergreen mortality scenario and the*
976 *control run for no beetle outbreak. Vegetation mortality for each sub-basin is calculated as the*
977 *percentage of evergreen patches multiplied by the mortality level of evergreen caused by beetles.*
978 *Long-term aridity is defined as temporally averaged (38 years) potential evapotranspiration*
979 *relative to precipitation.*
980



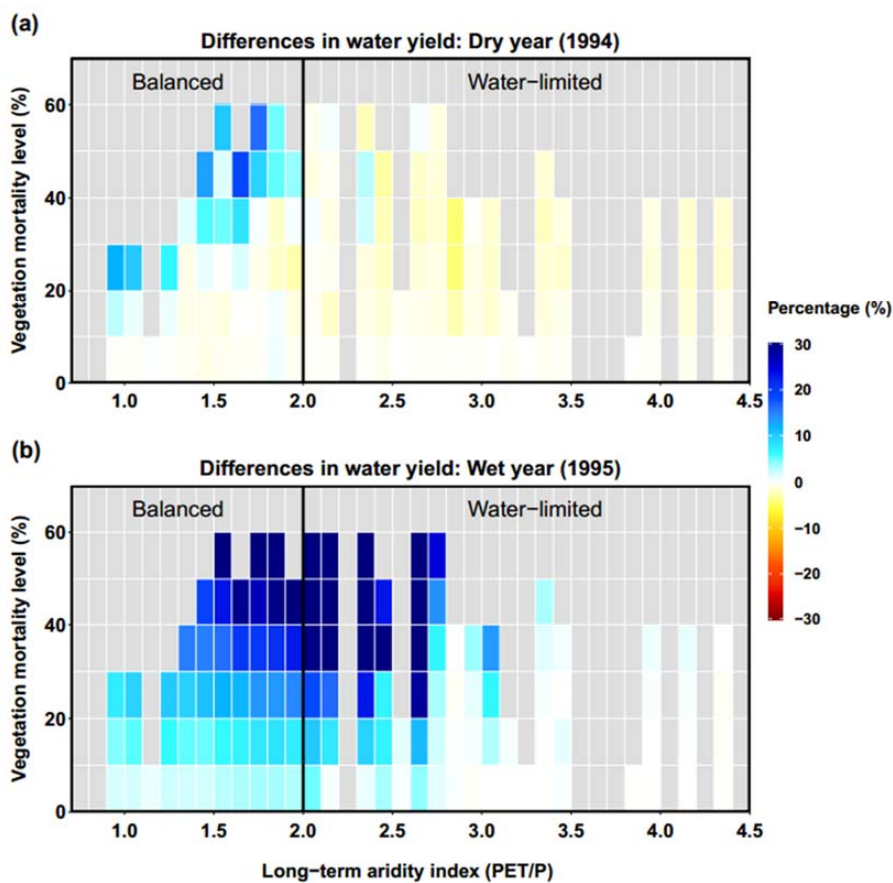
981

982 *Figure 8. Relationship among long-term aridity, vegetation mortality, and differences in*
983 *transpiration for a dry year (1994, a) and wet year (1995, b).*
984



985

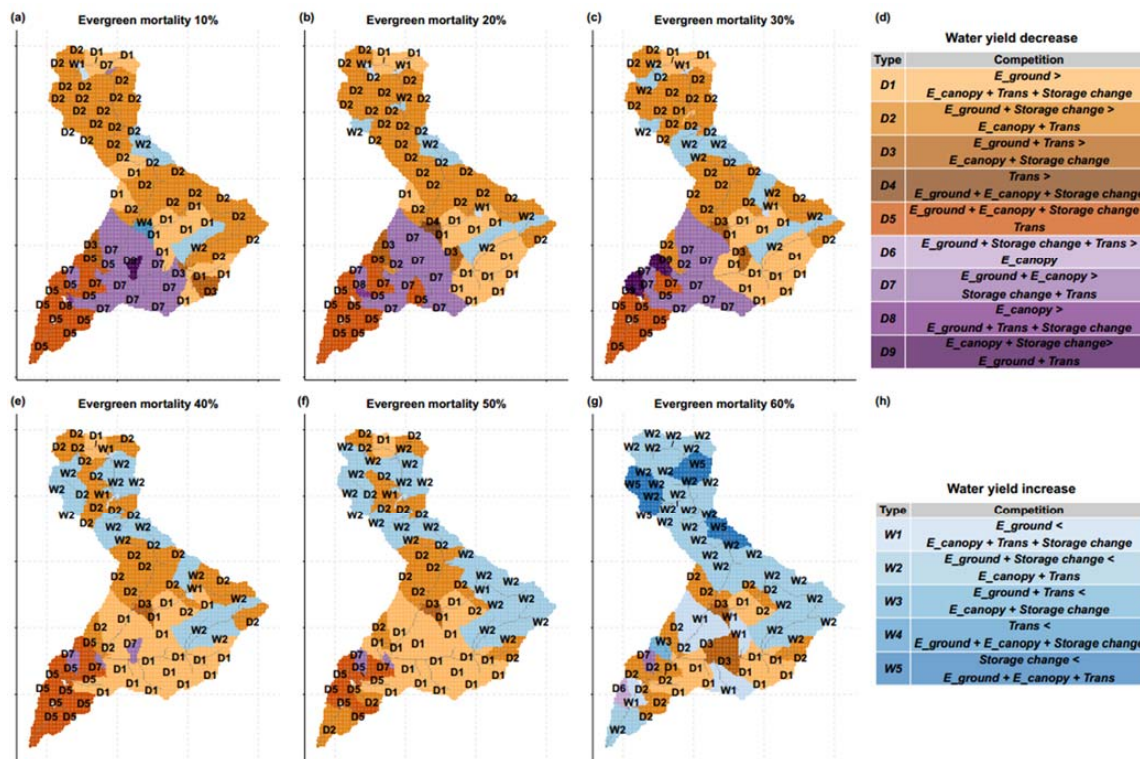
986 *Figure 9. Relationship among long-term aridity, vegetation mortality level and differences in ET*
987 *for a dry year (1994, a) and a wet year (1995, b).*
988



989

990 *Figure 10. Relationship among long-term aridity, vegetation mortality level and Differences in*
991 *water yield for a dry year (1994, a) and wet year (1995, b).*

992



993

994 *Figure 11. Water yield response types after beetle outbreak for different evergreen mortality*
 995 *scenarios compared with control scenario. D1 to D9 are water yield decrease types and W1 to*
 996 *W5 are water yield increase types. In panel D and H, the left side of each type are increasing*
 997 *fluxes that cause water yield decreases and the right side are decreasing fluxes that cause water*
 998 *yield increase. If the left side is larger than the right side, water yield increases, and vice versa.*
 999 *(Note: this mortality is evergreen mortality, which is different from vegetation mortality.)*

1000